

**Octreotide-targeted liposomes loaded with CPT-11 for the treatment
of medullary thyroid carcinoma**

Yuko Iwase

CONTENTS

GENERAL INTRODUCTION

CHAPTER 1

Octreotide-targeted liposomes loaded with CPT-11 for the treatment of medullary thyroid carcinoma *in vitro*

1. Introduction
2. Experimental section
 - 2.1. Materials
 - 2.2. Cell culture and cell preparation
 - 2.3. Preparation of Oct-targeted liposomes loaded with drug
 - 2.4. Cytotoxicity assay
 - 2.5. Analysis of cellular uptake of liposomes by flow cytometry
 - 2.6. Confocal laser scanning microscopy
 - 2.7. Cellular distribution by fluorescence microscopy
 - 2.8. *In vitro* drug release
 - 2.9. Statistical analysis
3. Results
 - 3.1. Characterization of Oct-targeted liposomes
 - 3.2. Effects of Oct surface density of Oct-targeted liposomes on cellular uptake
 - 3.3. Competitive inhibition study
 - 3.4. Drug release from liposomal CPT-11
 - 3.5. Cellular uptake of Oct-targeted liposomes loaded with CPT-11
 - 3.6. Effect on cytotoxicity of Oct-targeted liposomes
4. Discussion
5. Conclusions

CHAPTER 2

Octreotide-targeted liposomes loaded with CPT-11 for the treatment of medullary thyroid carcinoma xenografts

1. Introduction

2. Experimental section
 - 2.1. Materials
 - 2.2. Preparation of liposomal CPT-11
 - 2.3. Cytotoxicity assay
 - 2.4. Animals
 - 2.5. Antitumor effects
 - 2.6. Biodistribution in TT xenograft mice
 - 2.7. Distribution of liposomal CPT-11 in TT xenografts
 - 2.8. Conversion activity of CPT-11 by carboxylesterase
 - 2.9. Effect of octreotide-targeted liposomes on the PI3K/Akt/mTOR pathway in TT cells and TT tumors
 - 2.10. Statistical analysis
3. Results
 - 3.1. Size and zeta-potential of liposomes
 - 3.2. Therapeutic efficacy of liposomal CPT-11
 - 3.3. Biodistribution of liposomal CPT-11
 - 3.4. *In vitro* conversion of CPT-11 to SN-38
 - 3.5. Effects of Oct ligand of liposomes on growth inhibition and the phosphorylation of p70S6K
4. Discussion
5. Conclusions

CHAPTER 3

Liposomal everolimus for the treatment of lung carcinoma and medullary thyroid carcinoma
in vivo

1. Introduction
2. Experimental section
 - 2.1. Materials
 - 2.2. Cell cultures and cell preparations
 - 2.3. Preparation of liposomal everolimus
 - 2.4. Cytotoxicity assay
 - 2.5. Animal experiment
 - 2.7. Statistical analysis
3. Results

- 3.1. Size and zeta-potential of liposomes
- 3.2. Antitumor effect of liposomal everolimus *in vitro*
- 3.3. Antitumor effect on NCI-H446 tumor xenografts
- 3.4. Co-treatment efficacy with everolimus and CPT-11 *in vitro*
4. Discussion
5. Conclusions

SUMMARY

ACKNOWLEDGEMENTS

REFERENCES

List of Publication

1. Octreotide-targeted liposomes loaded with CPT-11 enhanced cytotoxicity for the treatment of medullary thyroid carcinoma: Iwase Y and Maitani Y., *Mol Pharm.* 8, 330-337 (2011). <presented in Chapter 1 of this dissertation>.
2. Dual functional octreotide-modified liposomal irinotecan leads to high therapeutic efficacy for medullary thyroid carcinoma xenografts: Iwase Y and Maitani Y., *Cancer Sci.* in press, <presented in Chapter 2 of this dissertation>.
3. Preparation and *in vivo* evaluation of liposomal everolimus for lung carcinoma and thyroid carcinoma: Iwase Y and Maitani Y., *Biol Pharm Bull.* accepted, <presented in Chapter 3 of this dissertation>.

Abbreviations

CL	Conventional non-PEGylated and non-targeted liposomes
CPT-11	Irinotecan
DDS	Dug delivery system
DSPC	Distearoylphosphatidylcholine
DXR	Doxorubicin
EPR	Enhancement permeability and retention
FBS	Fetal bovine serum
HPLC	High performance liquid chromatography
IC50	50% Growth-inhibitory concentration
IP-6	Phytic acid
MCF-7	Human derived breast cancer cell line
MTC	Medullary thyroid carcinoma
NCI-H446	Human derived small lung carcinoma cell line
Oct	Octreotide
Oct-CL	Octreotide-targeted liposome loaded with irinotecan
PBS	Phosphate-buffered saline
PEG	Methoxypolyethylene glycol
RES	Reticuloendothelial system
SL	PEGylated, sterically stabilized liposome
SN-38	7-Ethyl-10-hydrocamptothecin
SSTR	Somatostatin receptor
TT	Human derived medullary thyroid carcinoma cell line

GENERAL INTRODUCTION

Cancer is a serious medical and social problem throughout the world. In recent years in Japan, the number of cancer patients and cancer deaths has increased steadily and became the top of cause of death in 1981. According to statistics compiled by the Ministry of Health, Labor and Welfare, 344,105 people died of cancer in 2010. The major cause of cancer death among Japanese since 1993 has been lung cancer, followed by stomach and colon cancer. Conspicuous medical progress has led to some kinds of cancers being cured routinely. However, traditional medical approaches to cancer treatment have generally focused on cancers that occur in large numbers of affected individuals. Others cancers, particularly those that occur in small numbers of patients, often remain lacking in effective medical treatments. Therefore, research approaches toward rare cancers are very important from a social and medical viewpoint. Furthermore, efforts to generate therapies for rare cancers might clarify new viewpoints and provide insight into the treatment of common cancers.

Medullary thyroid carcinoma (MTC) is a rare endocrine tumor comprising a malignant neoplasm of calcitonin-secreting C cells of the thyroid gland and represents approximately 3-5% of all thyroid cancers.⁽¹⁾ MTC occurs in a sporadic form in about 75% of cases, and the remaining 25% are three familial forms; multiple endocrine neoplasia type IIA (MEN2A), multiple endocrine neoplasia type IIB (MEN2B), and familial MTC not associated with MEN (FMTC).⁽²⁾ The only effective treatment for MTC is surgical removal of the neoplastic tissue with central lymph node dissection.⁽³⁾ In the case of total thyroidectomy, however, lifelong hormone replacement therapy is necessary for patients, which decreases their quality of life. Most chemotherapy or radiotherapy for MTC has shown inconclusive results. The lack of effective systemic therapy for MTC shows the importance of developing new approaches for the treatment of this cancer. Vandetanib, an epidermal growth factor receptor-tyrosine kinase inhibitor, was approved by the FDA in April 2011 for the treatment of symptomatic progressive MTC in patients with unresectable (non-operable) locally advanced or metastatic disease.⁽⁴⁾ Thus, this positive approach for the treatment of MTC is attracting

significant attention.

Recently, therapeutic approaches for MTC using irinotecan (CPT-11, Fig. 1) have been reported in animal experiment.^{(5),(6)} CPT-11 is a water-soluble derivative prodrug of camptothecin and is converted to 7-ethyl-10-hydroxy-camptothecin (SN-38, Fig. 1), the active metabolite of CPT-11, by carboxyl esterase.^{(7),(8)} CPT-11 inhibits the resealing of single-strand DNA breaks mediated by topoisomerase I by stabilizing cleavable complexes and is a cell-cycle-specific drug.⁽⁹⁻¹¹⁾ Based on this, a long period of exposure to CPT-11 mediates a reduction in tumor cells, but treatment with CPT-11 is limited because of its short half-life and serious side-effects, such as bone-marrow suppression.⁽¹²⁾ Success in the treatment of MTC with CPT-11 requires selective delivery to tumor tissues and limited distribution to normal tissues.

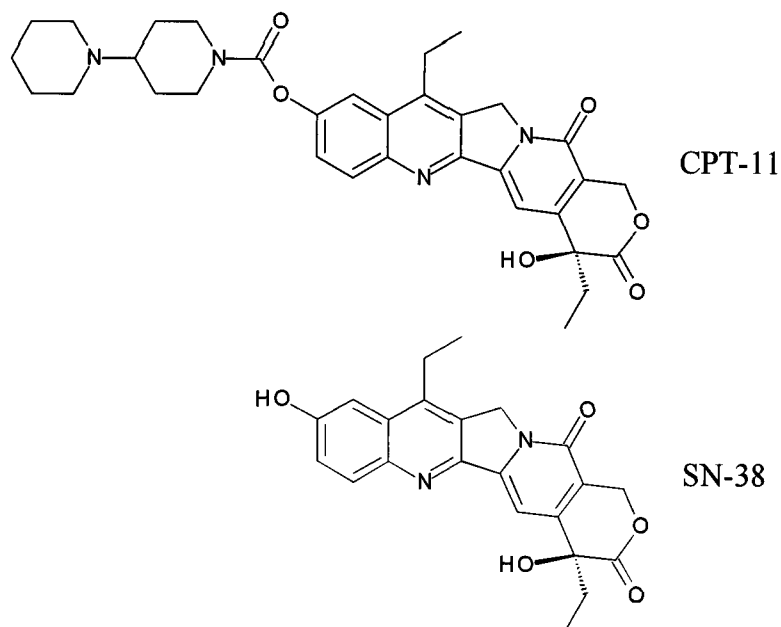


Figure 1. Chemical structures of irinotecan (CPT-11) and SN-38

Drug delivery systems (DDSs) such as micelles,⁽¹³⁾ microparticles⁽¹⁴⁾ and liposomes^{(15),(16)} have been investigated to increase selective drug delivery to specific tissues and tumor sites, in order to reduce drug adverse side-effects and to improve therapeutic efficacy via the enhancement permeability and retention (EPR) effect. Liposomes are defined as artificially prepared vesicles made from a lipid bilayer (Fig. 2A) and were first described as such by Bangham in 1961. More recently, liposomes have attracted considerable interest as a potential drug carrier.⁽¹⁷⁻¹⁹⁾ Liposomes are useful as a DDS tool owing to their unique properties: 1) hydrophilic drugs can be encapsulated inside liposomes and hydrophobic drugs can dissolve into the lipid membrane⁽²⁰⁾; 2) liposomes are biodegradable and biocompatible because they are mainly composed with phospholipids and cholesterol; 3) liposomal surface modification using ligands, such as antibodies,⁽²¹⁾ proteins⁽²²⁾ or sugar residues,⁽²³⁾ to increase targeted delivery is simple; and 4) changing liposomal size and/or surface charge to improve biodistribution is easy.

Particles, including liposomes, were shown to have very short circulation half-lives owing to rapid liposomal opsonization by plasma proteins and phagocytosis by fixed tissue macrophages of the reticuloendothelial system (RES).⁽²⁰⁾ To solve this problem, it was reported that liposomal membrane modification with methoxypolyethylene glycol (PEG)-derivative lipids (PEGylation) is effective (Fig. 2B).⁽²⁴⁻²⁶⁾

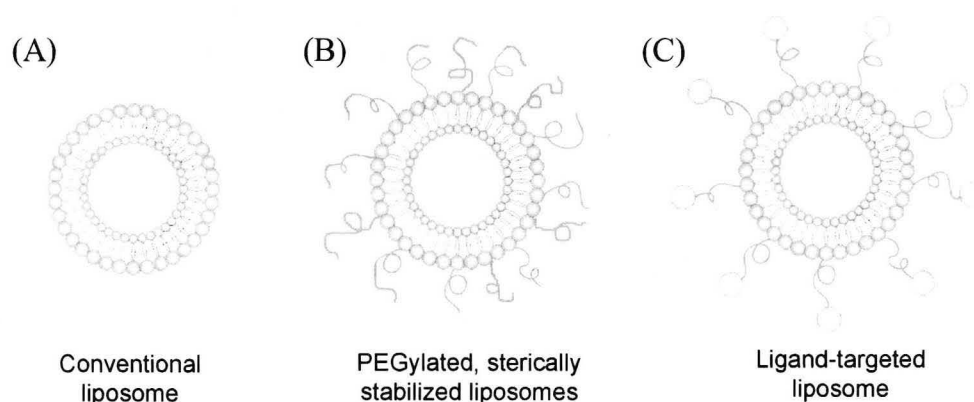


Figure 2. Conventional non-PEGylated and non-targeted liposomes (A), PEGylated, sterically stabilized liposomes (B) and ligand-targeted liposomes (C)

PEGylated liposomes provide a steric barrier against interaction with plasma proteins such as opsonins and lipoproteins. Because PEGylated liposomes have prolonged circulation half-lives, that of an encapsulated drug also increases with a corresponding increase in the duration of drug exposure; this strategy is able to evade rapid clearance by the RES.⁽²⁷⁾ Therapies utilizing this approach have now been licensed, including liposomal doxorubicin and antifungal agents.

A further strategy is known as “active targeting”, in which particles with ligands designed to interact with the tumor cells extravasate. This is therapeutically attractive because it involves bio-molecularly specific recognition, but no actively targeted agent has received regulatory approval to date except for monoclonal antibodies. To deliver drugs to specific cancer cell types, receptor-mediated endocytosis is a promising approach. Some cell-specific receptors, such as transferrin,⁽²²⁾ folate,⁽²⁸⁾ lipoprotein,⁽²⁹⁾ carbohydrate,⁽³⁰⁾ and somatostatin⁽³¹⁻³³⁾ receptors are utilized for the specific cell-targeted delivery of drugs (Fig. 2C).

Somatostatin receptors (SSTRs) belong to a seven transmembrane domain G-protein coupled receptor family (SSTR1, SSTR2, SSTR3, SSTR4, and SSTR5)⁽³⁴⁾ and can serve as a functional tumor-specific receptor. High levels of expression of SSTRs are generally detected in a variety of cancers, including human neuroendocrine tumor, pituitary adenomas, endocrine pancreatic tumors, gastrointestinal carcinoid, lung carcinoid and neuroblastoma (Table 1).^{(35),(36)} MTC tumors also express all the SSTR subtypes, and the MTC cell line TT overexpresses SSTR1, SSTR2 and SSTR5.⁽³⁷⁾ SSTR2 expression was significantly higher than the other SSTR subtypes in TT cells and was the most frequently detected subtype in human MTC.⁽³⁷⁻³⁹⁾

Octreotide (Oct) has high binding affinity to all SSTR subtypes,⁽⁴⁰⁾ especially SSTR2 ($K_d = 0.56$ nM).⁽³⁴⁾ Oct is an octapeptide analogue of natural somatostatin with markedly increased metabolic stability,⁽⁴¹⁾ resulting in an increased plasma-half-life of >1 h in rats⁽⁴¹⁾ and humans.⁽⁴²⁾ Oct has been marketed as a diagnostic agent⁽⁴³⁻⁴⁵⁾ and as an anticancer drug for neuroendocrine tumors: gastric cancer and pancreatic cancer.⁽⁴⁶⁻⁴⁸⁾ It was reported that Oct-modified liposomes loaded with anticancer drugs (cantharidin and dihydrotanshinone I) were efficacious in breast cancer and

gastric cancer, respectively, *in vitro*.⁽³¹⁻³³⁾ However, the therapeutic efficacy of these agents *in vivo* has not yet been reported.

Furthermore, it was reported that Oct alone could produce an anti-proliferative action to inhibit the phosphorylation of p70S6K in the PI3K/Akt/mTOR pathway in insulinoma cells (Table 1).⁽⁴⁹⁾ The PI3K/Akt/mTOR pathway is activated in many cancers.⁽⁴⁹⁾ Therefore, inhibition of this pathway maybe lead to the suppression of tumor growth. Moreover, the mTOR inhibitors rapamycin and rapamycin analogs are used clinically as anticancer drugs worldwide.⁽⁴⁹⁾ In Japan, everolimus, a rapamycin analog, was approved as an mTOR inhibitor for the treatment of renal cell carcinoma in 2009.⁽⁵⁰⁾

Table 1. Expression of somatostatin receptors (SSTRs) in neuroendocrine tumors and non-neuroendocrine tumors

Neuroendocrine tumors	Pituitary adenomas *
	Endocrine pancreatic tumors *
	Paragangliomas
	Pheochromocytomas
	Neuroblastomas *
	Medullary thyroid carcinoma *
Non-neuroendocrine tumors	Breast carcinoma *
	Renal carcinoma *
	Lung carcinoma *
	Liver carcinoma *
	Gastric cancer *
	Colorectal carcinoma *
	Ovarian carcinoma *
Prostatic carcinoma *	

* mTOR-activated cancer

MTC overexpresses SSTR2 especially and has sensitivity to CPT-11, while Oct has high binding affinity to SSTR2. Therefore, it is hypothesized that Oct-targeted liposomes loaded with CPT-11 might exhibit high therapeutic efficacy against MTC. The aim of this work is to prepare Oct-targeted liposome loaded with CPT-11 and liposomal mTOR inhibitor and evaluate their therapeutic the efficacy for MTC.

In Chapter 1, the characteristics of Oct-targeted liposome loaded with CPT-11 are evaluated in TT cells. In Chapter 2, the anticancer efficacy of the liposomes is evaluated in TT cells and in TT tumor xenografts. In Chapter 3, the anticancer efficacy of liposomal mTOR inhibitor is evaluated in TT cells and lung carcinoma xenografts.

CHAPER 1

Octreotide-targeted liposomes loaded with CPT-11 for the treatment of medullary thyroid carcinoma *in vitro*

1. Introduction

To date, there is no effective approach of treatment for MTC except for surgery. Chemotherapy for MTC had no inconclusive results. In animal study, therapeutic approaches for MTC using CPT-11 have been reported. However, CPT-11 therapy of MTC was failed due to low drug delivery efficacy to tumor site and severe side effect.⁽¹²⁾

For selective delivery of CPT-11 to medullary thyroid carcinoma cell line (TT cells), Oct-targeted liposome was used, because SSTR2 is known to overexpress on TT cells.

To generate formulation, in this chapter, I prepared Oct-targeted liposomes loaded with CPT-11 (Oct-CL) and investigated the characters such as size, surface charge, stability, and drug-release efficiency of the liposomes in TT cells. The ligand-modification-ratio optimization and the selective cellular uptake were investigated. The efficiency of Oct-CL as a selective drug carrier was evaluated by measuring the association of the liposomes by flow cytometry, confocal laser scanning microscopy and fluorescence microscopy. The cytotoxicity of the liposomes in TT cells was also measured.

2. Experimental section

2.1. Materials

CPT-11 was a kind gift from Yakult Co., Ltd. (Tokyo, Japan). Oct-poly(ethylene glycol) (PEG)₃₄₀₀-distearoylphosphatidylethanolamine (Oct-PEG-DSPE)⁽⁵¹⁾ was purchased from KNC Laboratories. Co., Ltd. (Kobe, Japan) (Fig. 3). Oct was purchased from Acris Antibodies GmbH (Herford, Germany). Distearoylphosphatidylcholine (DSPC) and methoxy-PEG₂₀₀₀-DSPE (PEG-DSPE) were purchased from the NOF Corp. (Tokyo, Japan). Chol, DXR hydrochloride, and Ham's F-12 medium were purchased from Wako Pure Chemical Industries, Ltd. (Osaka, Japan). Phytic acid (IP-6) solution was obtained from Nacalai Tesque Inc. (Kyoto, Japan). Fetal bovine serum (FBS) was purchased from Invitrogen Corp. (Carlsbad, CA, USA). Non-essential amino acids were purchased from MP Biomedicals. (Cleveland, OH, USA). Other reagents were of analytical or HPLC grade.

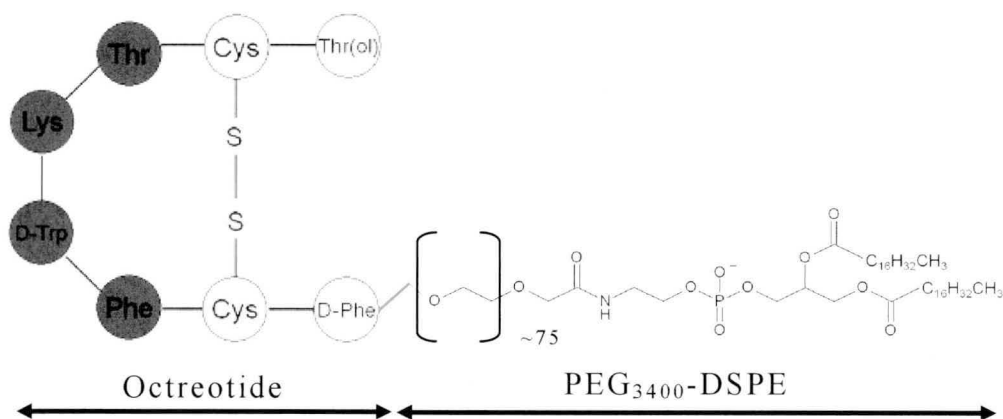


Figure 3. Chemical structure of Oct-PEG₃₄₀₀-DSPE (MW = ~5,200)

2.2. Cell culture and cell preparation

The TT cell was obtained from the European Collection of Cell Cultures (ECACC, Wiltshire, UK). This cell line was routinely maintained in Ham's F-12 medium supplemented with 10% heat-inactivated FBS at 37°C in

a humidified atmosphere containing 5% CO₂.

2.3. Preparation of Oct-targeted liposomes loaded with drug

Liposomes containing IP-6 (IP-6 liposomes) were formulated following previously described methods.⁽⁵²⁾ Briefly, DSPC and Chol at a molar ratio of 55:45 (80 mg/32 mg) were dissolved in ethanol. Ethanol was removed by rotary evaporation to a smaller volume, and 80 mM IP-6 solution adjusted to pH 6.5 using triethanolamine was added immediately, followed by sonication to decrease the size to approximately 150 nm. Then, the extra liposomal IP-6 suspension was exchanged for HBS buffer (20 mM HEPES, 150 mM NaCl, pH 7.4) by gel filtration chromatography using a Sephadex G50 column. The concentration of phospholipid (DSPC) of IP-6 liposomes was determined using a phospholipid C Test Wako (Wako Pure Chemical Industries, Ltd.), and then total lipid was calculated using DSPC and Chol at a molar ratio of 55:45. IP-6 liposomes were loaded with DXR or CPT-11 by incubation with CPT-11 (drug: total lipid = 0.6:1, wt/ wt) at 60°C for 60 min or with DXR (drug: total lipid = 0.2:1, wt/ wt) at 60°C for 25 min, and then quenched in ice for 5 min. Unincorporated CPT-11 or DXR was removed using a Sephadex G-50 column eluted with saline as the mobile phase.

Three types of liposomes were prepared; conventional non-PEGylated and non-targeted liposomes (CL), Oct-targeted liposomes (Oct-CL), and PEGylated, sterically stabilized liposomes (SL) (Fig. 2). Oct-CL was prepared by incubation of CL with an aqueous dispersion of 0.25-1.6 mol% Oct-PEG-DSPE with total lipids at 60°C for 20 min by the post insertion technique as reported previously.⁽⁵³⁾ Above 1.6 mol%, Oct-PEG-DSPE precipitates because of its insolubility in water. SL was prepared by incubation of CL with aqueous dispersion of 1.6 mol% PEG-DSPE in total lipids. CL modified with x mol% Oct-PEG-DSPE of total lipids are henceforth abbreviated as xOct-CL. For example, 0.25Oct-CL indicates liposomes with 0.25 mol% Oct-PEG-DSPE in total lipids (Table 2). Empty liposomes were prepared using the same protocol but without loading drug.

The mean diameter and zeta-potential of the resulting liposomes were determined using an ELS-Z2 (Otsuka, Electronics CO., Ltd. Osaka, Japan) at 25 ± 1°C after diluting the liposome suspension with water. Drug concentration in the liposomes was determined after disruption of liposomes

Table 2. Oct-PEG component (mol %) for each liposome formulation

Formulation	Oct-PEG ₃₄₀₀ -DSPE	PEG ₂₀₀₀ -DSPE
CL	0	0
0.25Oct-CL	0.25	0
0.8Oct-CL	0.8	0
1.0Oct-CL	1.0	0
1.2Oct-CL	1.2	0
1.4Oct-CL	1.4	0
1.6Oct-CL	1.6	0
SL	0	1.6

using 1% of Triton; DXR was determined using a UV-1700 PharmaSpec (Shimadzu, Kyoto, Japan) at 480 nm⁽⁵³⁾ and CPT-11 using a fluorometer (excitation wavelength 375 nm and emission wavelength 535 nm, Wallac ARVO SX1420 multi-label counter, PerkinElmer Japan, Yokohama, Japan).⁽⁵³⁾ No drug leaked out from the liposomes during the Oct-PEG-DSPE insertion procedure. The final Oct concentration after modification of the liposomes was determined using an Oct-EIA kit (Peninsula Laboratories, LLC, San Carlos, CA, USA) after disruption of the liposomes by dilution 1:1,000 in 1% Triton. About 84%, 85%, and 70% of Oct ligand was inserted into 0.25Oct-CL, 0.8Oct-CL, and 1.6Oct-CL, respectively.

2.4. Cytotoxicity assay

TT cells were seeded onto 96-well plates at a density 10^4 cells/well for 72 h before addition of the drug. Culture medium was replaced with fresh medium containing various concentrations of liposomal CPT-11, free CPT-11 or empty liposomes. After 96-h incubation at 37°C, the cells were washed with PBS three times and cultured with fresh medium for 48 h. Then, cell viability was determined using a WST-8 test (Dojindo Laboratories, Kumamoto, Japan). All measurement was carried out in quadruplicate. The 50% growth-inhibitory concentration (IC₅₀) was calculated using the bootstrap method.⁽⁵⁴⁾

2.5. Analysis of cellular uptake of liposomes by flow cytometry

Cells were seeded 6-well plates at a density 10^4 cells/well for 72 h before addition of the drug. Cells were incubated with medium (2 ml/well) containing 0.25Oct-CL, 0.8Oct-CL, 1.0Oct-CL, 1.2Oct-CL, 1.4Oct-CL, 1.6Oct-CL, or SL at a concentration of 50 μg of DXR/ml for 1 or 2 h. In flow cytometry and confocal laser scanning microscopy studies, as described below, DXR was used instead of CPT-11 because CPT-11 is not excited at 488 nm. Subsequently, cells were washed three times with PBS (pH 7.4) to remove unbound liposomes, and the cellular uptake of liposomes was analyzed using a FACS Calibur flow cytometer (Becton Dickinson, CA, USA) equipped with a 488 nm argon ion laser and using CELL Quest software (Becton-Dickinson Immunocytometry System, CA, USA). A total of 10,000 events per sample were analyzed. The autofluorescence of cells was taken as a control. The cells were incubated without liposomes.

In competitive inhibition experiments, a 20-fold molar excess of free Oct (84 nmol/ml medium) was added to 1.6Oct-CL loaded with DXR. The medium in each well (2 ml) contained 50 μg of DXR/ml, 4.2 nmol of Oct originating from 1.6Oct-CL/ml, and 112 μg of phospholipid/ml. A two-volume excess of empty 1.6Oct-CL or SL (258 μl) was added to 1.6Oct-CL loaded with DXR. Because all liposomes have a lipid concentration 194 μg of phospholipid/ml, the final concentration of phospholipid in medium was 582 $\mu\text{g}/\text{ml}$. This was nearly the maximum tolerated concentration because greater than 0.6 mg of phospholipid/ml induces cytotoxicity. The cells were incubated at 37°C for 2 h.

2.6. Confocal laser scanning microscopy

Cells were seeded in 6-well plates at a density 10^4 cells/well for 72 h before addition of the drug. Cells were washed three times with PBS and then incubated with 1.6Oct-CL loaded with DXR in the presence or absence of a two-volume excess of empty 1.6Oct-CL or SL for 2 h at 37°C, as described above. After incubation, the cells were washed three times with PBS and fixed with 10% formaldehyde in PBS at room temperature for 15 min. Then, the cells were washed two times with PBS and coated with Aqua Poly/Mount (Polyscience, Warrington, PA, USA) to prevent fading and covered with

coverslips. The fixed cells were observed using a Radiance 2100 confocal laser scanning microscope (Bio-Rad, Hercules, CA, USA) with an excitation wavelength at 488 nm and an emission wavelength at 560 nm utilizing a LP560 filter.

2.7. Cellular distribution of liposomal CPT-11 observed by fluorescence microscopy

Cells were seeded 35 mm glass dishes at 10^4 cells/dish for 72 h before addition of the drug. Cells were treated with medium containing 1.6Oct-CL loaded with CPT-11 for 2 h at 37°C. After incubation, the cells were fixed and coated as described above. Cells were examined using an inverted microscope, ECRIPS TS100 (Nikon, Tokyo, Japan) with an Epi-Fluorescence Attachment (Nikon, Tokyo, Japan) a utilizing a UV1A filter.

2.8. *In vitro* drug release

The release of the drug from liposomes into phosphate-buffered saline (PBS, pH 7.4) was monitored by a dialysis method. Dialysis was carried out at 37°C under sink conditions using seamless cellulose tube membranes Spectra/Por CE (MWCO 2000, Spectrum Laboratories, Inc., Rancho Dominguez, CA, USA). The initial concentration of CPT-11 was 500 µg/ml. The sample volume in the dialysis bag was 1 ml and the sink solution was 200 ml. After various time intervals, aliquots were withdrawn and the CPT-11 concentrations were analyzed as described above.

2.9. Statistical analysis

Data are expressed mean \pm S.D. The statistical significance of data was evaluated using Student's *t* test. $P < 0.05$ was considered as significant.

3. Results

3.1. Characterization of Oct-targeted liposomes

Liposome size and zeta-potential of CL, Oct-CL and SL are listed in Table 3. The average diameter of prepared liposomes was approximately 134–154 nm with a narrow, monodisperse distribution (less than 0.2 polydispersity indexes). As the Oct concentration increased from 0 to 1.6 mol%, the zeta-potential of liposomes decreased. The Oct amount of each Oct-CL was more than 70% of the theoretical values. The loading efficiencies of CPT-11 were approximately > 82% in all liposomes except CL (data not shown). The average diameter and amount of CPT-11 loaded in all types of liposomes did not change for at least 1 month at 4°C in the dark (data not shown).

Table 3. Size and zeta-potential of Oct-targeted liposomes

Formulation	Size (nm)		Zeta-potential (mV)	
CL	151.9	± 5.5	-5.1	± 0.1
0.25Oct-CL	141.3	± 6.1	-11.2	± 3.5
0.8Oct-CL	141.6	± 9.4	-17.8	± 6.9
1.0Oct-CL	153.9	± 6.2	-18.1	± 4.3
1.2Oct-CL	134.2	± 5.4	-15.3	± 1.9
1.4Oct-CL	147.6	± 2.4	-17.3	± 4.7
1.6Oct-CL	136.6	± 3.2	-19.5	± 1.3
SL	144.7	± 1.6	-20.1	± 1.6

Note; Mean ± S.D. (n = 3).

3.2. Effects of Oct surface density of Oct-CL on cellular uptake

I examined the selectivity of Oct-CL for delivery into TT cells, which highly overexpress SSTR2, by flow cytometry. As shown in Fig. 4, the mean fluorescence intensities of 0.8Oct-CL, 1.0Oct-CL, 1.2Oct-CL, 1.4Oct-CL and 1.6Oct-CL were approximately 1.1-fold, 1.2-fold, 1.2-fold, 1.7-fold and 1.7-fold greater than for SL, respectively, after a 2 h incubation. The cellular uptake of free DXR was ~3 times higher than that of 0.25Oct-CL (data not shown). When paying attention to the effects of the Oct surface density of liposomes on cellular association, a higher Oct surface density, more than 1.4 mol% of liposomes was more effectively associated with TT cells.

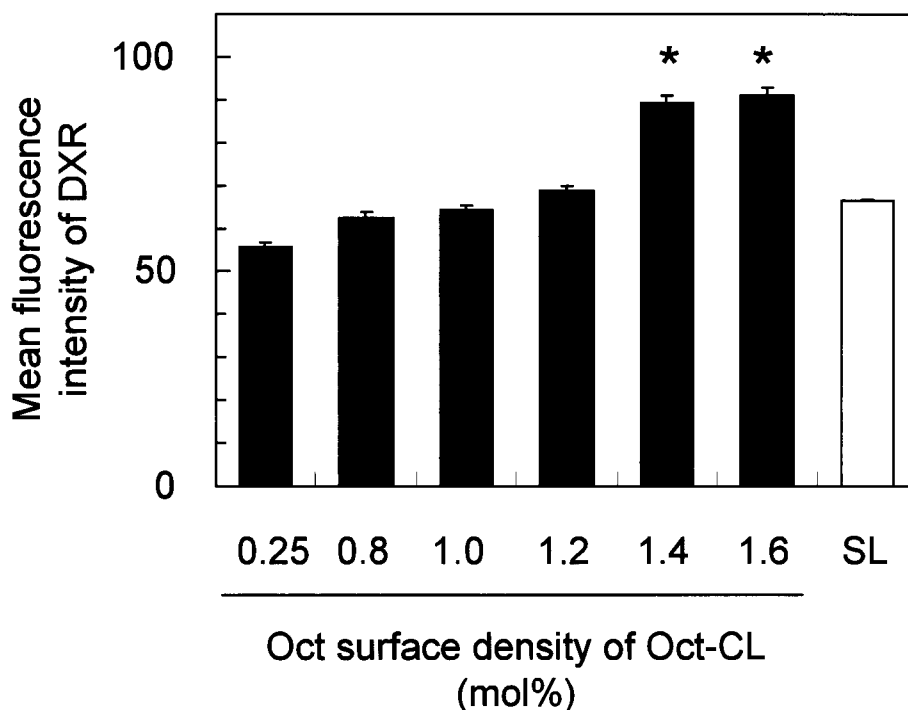


Figure 4. Effect of Oct surface density on cellular association of Oct-CL

DXR-loaded liposomes modified with various Oct-PEG-DSPE concentrations (mol%) were incubated with TT cells at 50 μ g/ml DXR for 2 h at 37 $^{\circ}$ C.

Each value represents the mean \pm S.D. (n = 3).

* Differences are statistically significant from SL at $P < 0.05$.

The fluorescence intensities of 1.6Oct-CL after a 2 h-incubation increased 2-fold more than after 1 h, whereas that of SL did not increase (data not shown). This finding indicated that the cellular association of Oct-CL increased in an incubation time-dependent manner, but that of SL was not. From this result, 1.6Oct-CL was used in the following experiments as Oct-CL, and SL was used as a control for the 2 h incubation.

3.3. Competitive inhibition study

First, to investigate the cellular association of Oct-CL *via* SSTR, a competitive inhibition study was performed using free Oct as a competitive inhibitor. In the presence of a 20-fold excess of free Oct (84 nmol/ml medium) with 2 h incubation, a competitive effect, a decrease of cellular uptake of Oct-CL, was not observed (Fig. 5).

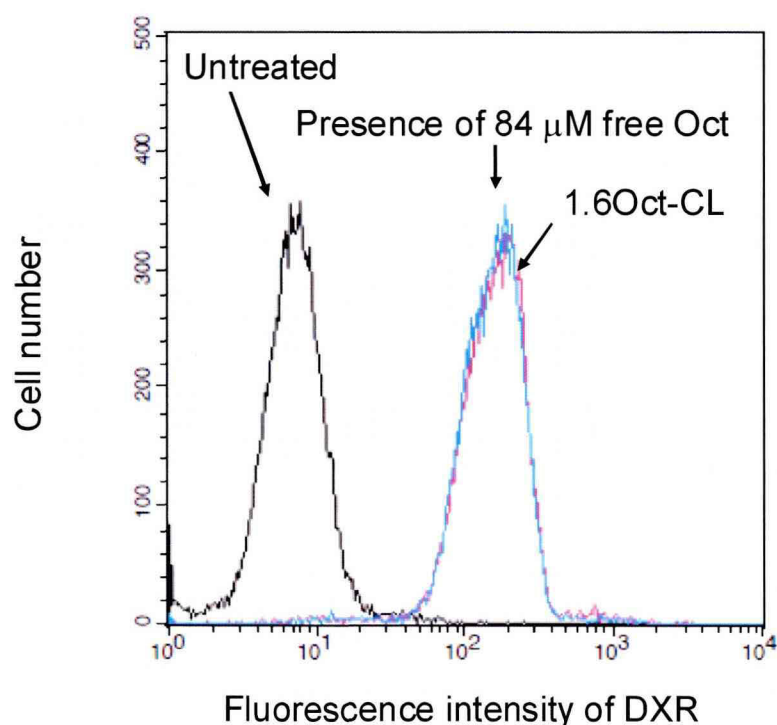


Figure 5. Association of Oct-CL loaded with DXR with TT cells in the presence or absence of free Oct by flow cytometry. 1.6Oct-CL loaded with DXR was incubated in the presence of a 20-fold excess of free Oct (84 μM) at 50 μg/ml DXR for 2 h at 37°C. Untreated indicates auto fluorescence of untreated cells.

Next, I tried to use Oct-CL without drug loading (empty Oct-CL) as a competitive inhibitor, because addition of drug-loaded liposomes has the possibility of increasing the cytotoxicity due to DXR. Fig. 6A illustrates the scheme of the competitive cellular association of Oct-CL loaded with DXR with empty Oct-CL. The cellular uptake of Oct-CL loaded with DXR in the presence of two excess volumes of empty Oct-CL (i) was compared with that of empty SL (ii) by flow cytometry (Fig. 6B) and confocal microscopy (Fig. 7). As shown in Figure 6B, the mean fluorescence intensities of DXR loaded with Oct-CL in the presence of empty Oct-CL decreased by approximately half compared with in the presence of empty SL. This finding indicated that the cellular uptake of Oct-CL loaded with DXR was blocked significantly by empty Oct-CL compared with empty SL.

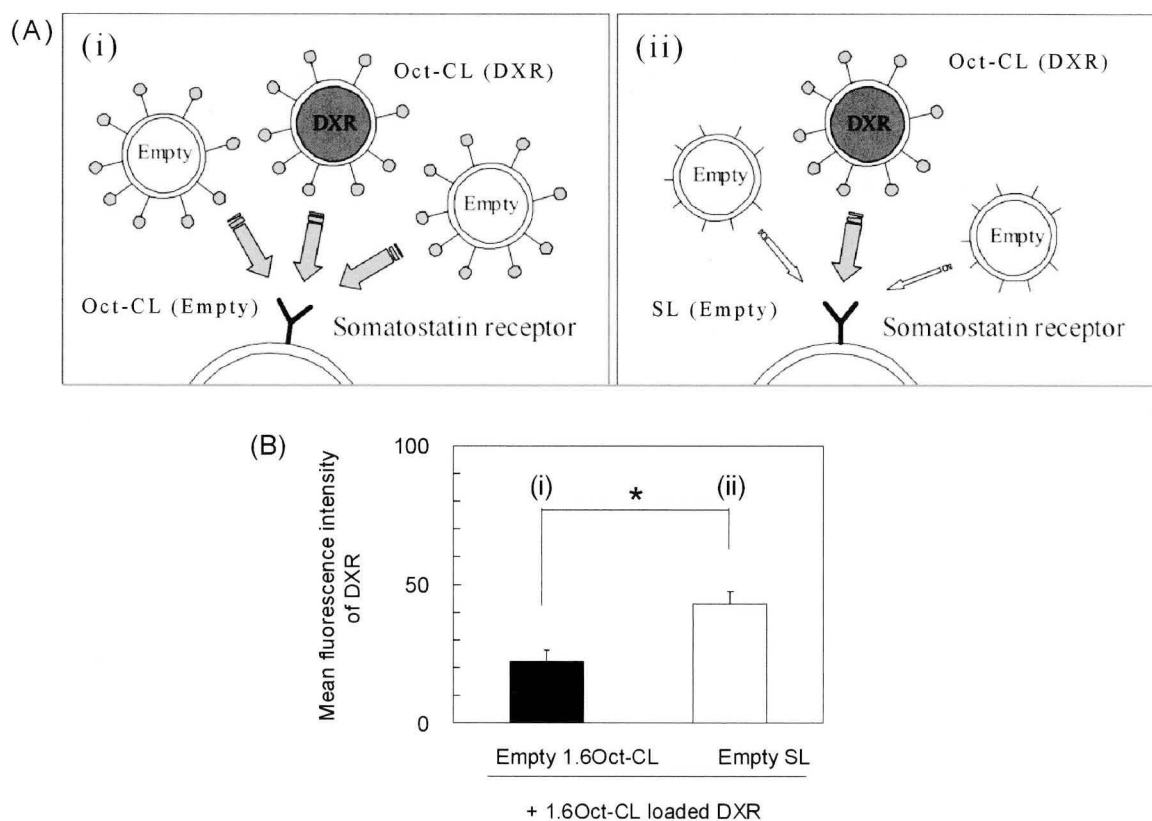


Figure 6. Scheme (A) and DXR fluorescence (B) of cellular association of 1.6Oct-CL loaded with DXR with TT cells in the presence of two excess volumes of empty 1.6Oct-CL (i) or empty SL (ii) for 2 h at 37°C by flow cytometry. Each value is the mean \pm S.D. for three experiments. * Differences are statistically significant at $P < 0.05$.

To confirm differences in the cellular uptake of Oct-CL loaded with DXR in the presence of empty Oct-CL or SL, intracellular localizations were observed by confocal microscopy (Fig. 7). The presence of empty Oct-CL decreased the localization of DXR-loaded Oct-CL in the nucleus (red fluorescence of DXR) compared with that of empty SL, corresponding to the results of Fig. 6B (i) and (ii), respectively.

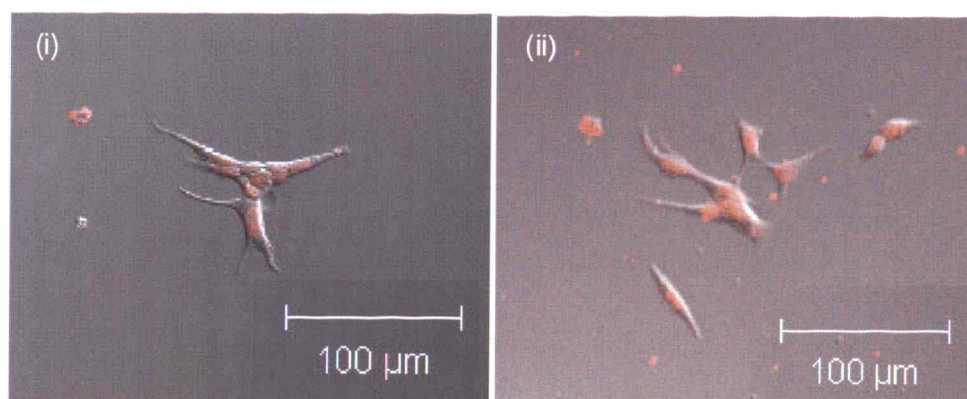


Figure 7. Effects of empty 1.6Oct-CL (i) or SL (ii) on the cellular association of 1.6Oct-CL loaded with DXR with TT cells determined by confocal microscopy
The experimental conditions were the same as for Figure 6B.
Scale bar denotes 100 μm .

3.4 Drug release from liposomal CPT-11

Before the investigation of cellular uptake of Oct-CL and SL, the release of drug from each liposome was examined. The profiles of CPT-11 release versus time are presented in Fig. 8. Both Oct-CL and SL showed slow drug release, about 17% drug release for 24 h in PBS at 37°C. There were no significant differences between Oct-CL and SL in drug release at each time point. This result suggested that 1.6mol% Oct-modification did not affect drug release from liposomes.

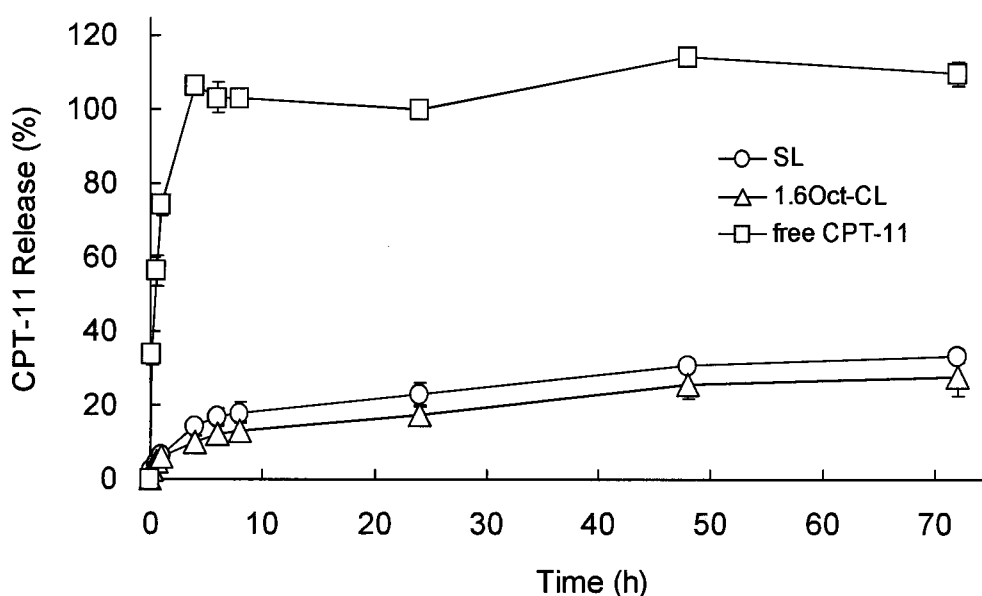


Figure 8. Percentage of CPT-11 released from 1.6Oct-CL and SL as a function time at 37°C

Each value represents the mean \pm S.D. of three experiments.

3.5. Cellular uptake of Oct-CL

Next, I tried to observe the cellular distribution of liposomes loaded with CPT-11 by fluorescence microscopy (Fig. 9). TT cells were incubated with Oct-CL loaded with CPT-11 for 2 h at 37°C. Blue fluorescence due to CPT-11 (Fig. 9A) was observed weakly in Oct-CL loaded with CPT-11 at the same location as TT cells (Fig. 9B). This finding indicated that Oct-CL loaded with CPT-11 was taken up into the cells as well as Oct-CL loaded with DXR.

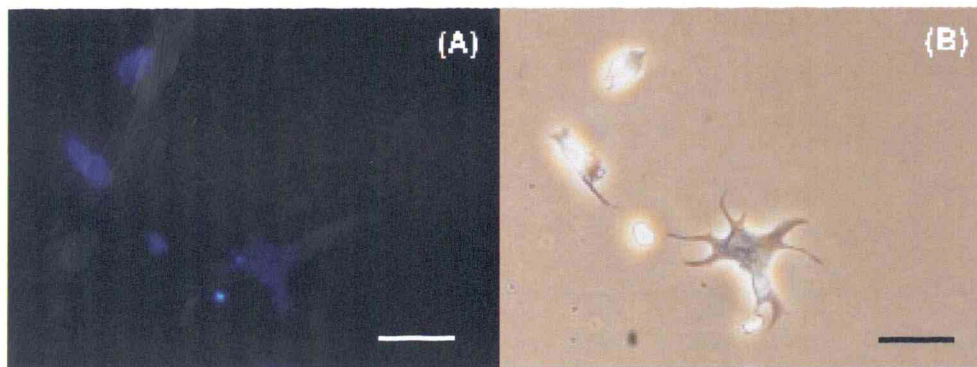


Figure 9. Cellular uptake of liposomal CPT-11 observed by fluorescence microscopy

TT cells were incubated with 1.6Oct-CL loaded with CPT-11 for 2 h at 37°C. Blue fluorescence; location of CPT-11.

Dark field (A), and bright field (B). Scale bar, 50 μm.

3.6. Effect on cytotoxicity of Oct-targeted liposomes

To evaluate the cellular uptake of Oct-CL loaded with CPT-11, the cytotoxicity with TT cells was measured using a WST-8 assay. The doubling time of TT cells is 83 h; therefore, a 96-h incubation was set in this experiment. As shown in Table 4, free CPT-11, Oct-CL, and SL increased cytotoxicity in an incubation time-dependent manner. Free CPT-11 showed higher cytotoxicity than liposomal CPT-11 with 48-h and 72-h incubations. After a 96-h incubation, the IC₅₀ value of Oct-CL was the lowest ($1.05 \pm 0.47 \mu\text{M}$), whereas free CPT-11 ($3.76 \pm 0.61 \mu\text{M}$) and SL ($3.05 \pm 0.28 \mu\text{M}$), gave the similar cytotoxicity results. Therefore cytotoxicity of Oct-CL loaded with CPT-11 may be due to cellular uptake of liposomal CPT-11. In addition, $8.4 \mu\text{M}$ Oct originating from empty 1.6Oct-CL significantly decreased TT cell viability to 60% after a 96-h incubation compared with empty SL (corresponds to the amount of PEG-DSPE of Oct-CL) (Fig. 10). In the case of more than about $12 \mu\text{M}$ Oct using 1.6 Oct-CL (total lipid 1.02 mM), cytotoxicity of liposomes was observed due to the lipids. On the other hand, cytotoxicity of free Oct was not observed independent of the Oct concentration (data not shown).

Table 4. IC₅₀ of free CPT-11 and liposomes loaded with CPT-11 on TT cells after various incubation times

Formulation	IC ₅₀ (μM)		
	48 h	72 h	96 h
Free CPT-11	7.43 ± 6.73	5.10 ± 1.85	3.76 ± 0.61
1.6Oct-CL	29.05 ± 19.40	8.72 ± 1.14	1.05 ± 0.47*
SL	22.50 ± 19.50	8.65 ± 2.26	3.05 ± 0.28

Note; Mean ± S.D. (n = 4).

*, Differences are statistically significant from SL at $P < 0.05$.

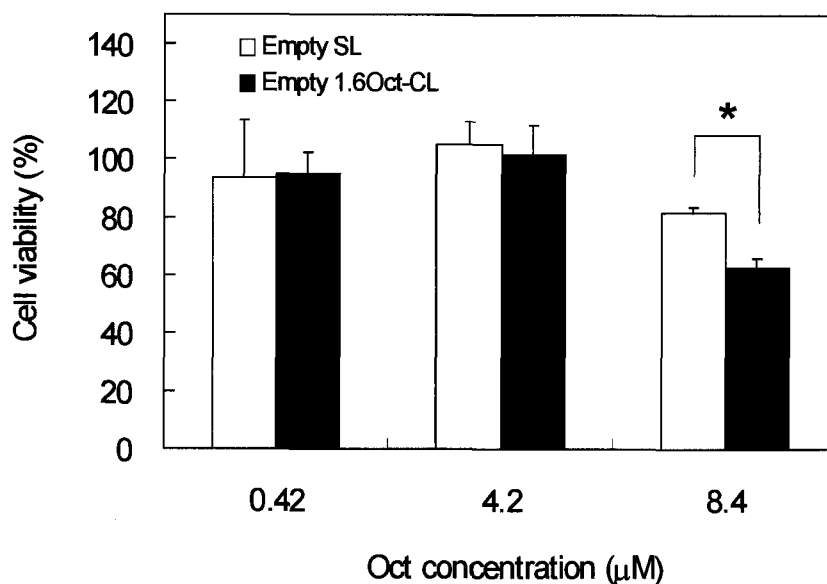


Figure 10. Effect of Oct concentrations on cell viability of 1.6Oct-CL compared with SL

TT cells were incubated with empty 1.6Oct-CL or empty SL for 96 h at 37°C.

* Differences are statistically significant at $P < 0.05$.

Each value represents the mean ± S.D. (n=4).

4. Discussion

In this chapter, I prepared Oct-CL loaded with CPT-11 and demonstrated that high Oct-surface-density significantly increased the cellular association of Oct-CL *via* SSTR and approximately 2-fold higher cytotoxicity when compared with free CPT-11 and PEGylated liposomes (SL) with TT cells using a 96-h exposure period. Recently, it was reported that 0.5 mol% Oct-modified liposomes, loaded with anticancer drug were selectively taken by the cells and were effective for the treatment of SSTR-positive breast cancer, gastric cancer and lung carcinoma.⁽³¹⁻³³⁾ In the case of transferrin-targeted liposomes modified with transferrin-PEG-DSPE, the cellular uptake of liposomes was dependent on the concentration of transferrin-PEG-DSPE.⁽⁵⁵⁾ Therefore, I increased the concentration of Oct-PEG-DSPE in the liposomes and found that the cellular uptake of the Oct-CL increased more effectively with high Oct-surface-density, more than 1.4 mol% (Fig. 4).

There were two striking observations in this study. First, the cellular uptake of Oct-CL was significantly inhibited by empty Oct-CL. The competitive inhibition study of cellular uptake of ligand-modified liposomes was generally done using excess free ligands, not using ligand-liposomes such as Oct-CL. For example, it was reported that the cellular uptake of transferrin-targeted liposomes was inhibited by 20-fold excess transferrin.⁽⁵⁵⁾ In this study, 20-fold excess free Oct did not inhibit the cellular uptake of Oct-CL (data not shown). In the competitive inhibition study *via* SSTR, 100-, 1,000- or 1,000,000-fold excess of Oct was used.⁽⁵⁶⁻⁵⁸⁾ These experiments had a very high cost, and Oct has been reported to be used as an anticancer drug.^(59, 60) This information suggested that the use of such an excess Oct was not suitable for competition of the cellular uptake of Oct-CL because of increases in cytotoxicity. Gabizon *et al.*⁽⁶¹⁾ reported that liposome binding is multivalent, in other words, several ligands contribute to cellular uptake, and the overall affinity for the target cell is the product of the individual affinities of the ligands participating in binding. It could be predicted that the affinity of free Oct and Oct-CL to SSTR are not the same. In this regard, I used empty Oct-CL and empty SL as a competitive inhibitor and as a control, respectively (Fig. 6). The cellular uptake of 1.6Oct-CL loaded with drug (Oct concentration 7.2 μ M) was inhibited significantly by empty Oct-CL with 14.4

μM Oct, compared with empty SL. This finding indicated that Oct-CL associated *via* SSTR, and the affinity of Oct-CL to SSTR was substantially higher than that of free Oct.

Second, the cytotoxicity Oct-CL loaded with CPT-11 incubated for 96 h was higher than that of free CPT-11 and SL loaded with CPT-11. The cytotoxicity of free CPT-11 increased in an incubation-time dependent manner from 24 h to 96 h in TT cells, as reported previously.⁽⁶²⁾ The long incubation times may lead to metabolization of CPT-11 to SN-38; the active form of CPT-11 in TT cells. As a result, the cytotoxicity of free CPT-11 after the 96-h incubation increased six-fold compared with at 48 h, and that of Oct-CL increased ~ 25 times, resulting in the highest cytotoxicity among free CPT-11 and SL. These findings suggested that a long incubation time caused CPT-11 release from the taken liposomes, which was converted to the active form SN-38, and consequently increased the cytotoxicity. The receptor-mediated endocytosis mechanism of Oct-CL significantly facilitated cellular uptake and the cytotoxic potential of CPT-11 compared with SL.

The question remains why 1.6Oct-CL showed higher cytotoxicity than free CPT-11, which freely diffuses into cells. Empty 1.6Oct-CL as a control of 1.6Oct-CL (correspond to $4.2 \mu\text{M}$ of Oct-PEG-DSPE) at 96-h incubation in the cytotoxicity experiments was shown to have no effects (Fig. 10). However, empty 1.6Oct-CL showed higher cytotoxicity than empty SL liposomes modified with PEG-lipid corresponded to Oct-PEG-lipid of 1.6Oct-CL at 96-h incubation, at the concentration where free Oct did not show cytotoxicity, suggesting that Oct as a ligand showed cytotoxicity.

With regard to Oct activity, Oct was reported to produce an anti-proliferative action in insulinoma cells and pituitary tumor cells.^(60, 61) These findings suggested that Oct might show an anti-proliferative effect in TT cells. From this, Oct may cause empty Oct-CL to show a stronger cytotoxicity than empty SL because Oct-CL were taken up effectively *via* SSTR. However, further experiments are needed to clarify these points *in vitro*.

In an *in vitro* study, Oct increased selectively the cellular association of liposomal CPT-11 (Fig. 4), and empty 1.6Oct-CL decreased the viability of TT cells (Fig. 10). These findings suggested that Oct-modification of liposomal CPT-11 improved therapeutic efficacy for MTC *in vitro*.

5. Conclusion

In Chapter 1, the present study showed that higher concentrations of modified Oct-CL associated effectively with TT cells *via* the somatostatin receptor and had higher cytotoxicity than free CPT-11 or PEGylated liposome, SL. These findings indicated that Oct-targeted liposomes loaded with CPT-11 might offer considerable potential for MTC chemotherapy because cytotoxicity of both CPT-11 and Oct was enhanced by effective cellular uptake *via* the somatostatin receptor.

CHAPER 2

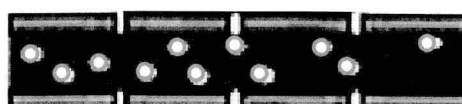
Octreotide-targeted liposomes loaded with CPT-11 for the treatment
of medullary thyroid carcinoma xenografts

1. Introduction

As described in Chapter 1, 1.6 mol% Oct modified liposomes loaded with CPT-11 (Oct-CL) had a potential of therapeutic treatment for MTC. Therefore, I examined the therapeutic efficacy of the liposomes for MTC xenografts. It is known that liposomal drug can improve drug delivery efficiency compared with free drug. It is also well known that intravenously injected PEGylated liposomes, SL can passively accumulate into tumor tissue due to the EPR effect (Fig. 11).⁽⁶⁵⁾ Therefore, the antitumor effects Oct-CL were compared with these of free CPT-11, non-PEGylated liposome loaded with CPT-11 (CL), and SL to clarify whether the active-targeting Oct-CL was superior to CL and the passive targeting SL.

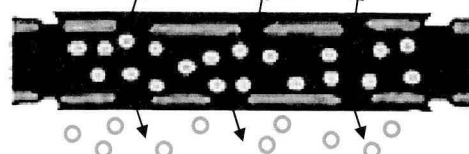
It was also observed in Chapter 1, that non-drug loaded Oct-CL; empty Oct-CL, showed higher cytotoxicity compared with empty SL in TT cells (Fig 10). To gain more insight into tumor suppression, I examined the mechanism of cytotoxicity of the Oct ligand. In this Chapter, the function of Oct ligand in Oct-CL from viewpoints of therapeutic efficacy and the biodistribution and conversion of CPT-11 in MTC tumor xenografts after the intravenously injection of Oct-CL or SL, were observed. Furthermore, the cytotoxicity mechanism of Oct ligand using empty Oct-CL *in vitro* and *in vivo*, was assessed.

(A) Normal vasculature



EPR effect (-)

(B) Tumor vasculature



EPR effect (+)

Figure 11. Enhancement permeability and retention (EPR) effect in normal vasculature (A) and tumor vasculature (B)

2. Experimental section

2.1. Materials

CPT-11, DSPC, PEG-DSPE, IP-6 and Chol were the same ones in Chapter 1. SN-38 was purchased from Wako Pure Chemical Industries, Ltd. (Osaka, Japan). Other reagents were of analytical or HPLC grade.

2.2. Preparation of liposomal CPT-11

Three types of liposomal CPT-11 (CL, SL and Oct-CL) were prepared. Liposomal preparation methods were described in Experimental section of Chapter 1. Liposomes were incubated with 1.6 mol% Oct-PEG-DSPE for Oct-CL or 1.6 mol% PEG-DSPE for SL at 60°C for 25 min.⁽⁶⁶⁾ Empty liposomes were prepared using the same protocol but without loading drug.

2.3. Cytotoxicity assay

Cytotoxicity on TT cells (human MTC cell line) was carried out using free Oct or empty liposomes. Cells were incubated for 48 h at the different concentrations of free Oct, empty liposomes in the presence or absence of 1.5 μ M CPT-11, which corresponded to one-tenth of the 50% growth-inhibitory concentration.⁽⁶⁶⁾ Lipid amount of empty SL corresponded to that of empty Oct-CL. Cell viability was measured by the same protocol described in Chapter 1.

2.4. Animals

All animal experiments were performed with approval from the Institutional Animal Care and Use Committee at Hoshi University. TT cells (1×10^7) were inoculated subcutaneously into female ICR nu/nu mice (6 weeks of age, Oriental Yeast Co., Ltd., Tokyo, Japan).

2.5. Antitumor effects

When the average tumor volume was approximately 100 mm³, Experiment 1; CL or Oct-CL was injected intravenously at a dose of 10 mg CPT-11/kg twice at three-day intervals (24.1 mg lipid/kg/injection). Free CPT-11 (30 mg CPT-11/kg) and saline were injected intravenously three times at three-day intervals. The data of free CPT-11-treated and saline-treated mice were referring to our previous data.⁽⁶²⁾ Experiment 2; Oct-CL or SL was

injected intravenously at a dose of 10 mg CPT-11/kg in two times at three-day intervals (23.9 mg lipid/kg/injection). Experiment 3; Empty Oct-CL or empty SL was injected intravenously (23.5 mg lipid and 867 nmol Oct/kg/injection, corresponding to Oct ligand amount of 1.6Oct-CL) in two injections at three-day intervals. SSTR2-mRNA was detected in TT tumor xenografts by RT-PCR analysis (data not shown).

Tumor volume and body weight were measured for individual animals. Tumor volume was calculated using the following equation: $\text{volume} = 1/2 ab^2$, where a is the long diameter and b is a short diameter. The mean increase in life span (%ILS) was calculated using the formula; $100 \times \{(\text{median day of death in treated tumor-bearing mice}) - (\text{median day of death in control tumor bearing-mice})\} / (\text{median day of death in control tumor bearing-mice})$.

2.6. Biodistribution in TT xenograft mice

When the average tumor size reached approximately 100 mm^3 , mice were injected with Oct-CL or SL intravenously at a dose of 10 mg CPT-11/kg. At 6 h and 24 h after a single injection, blood was collected. Tumor, liver, kidneys, lung and spleen were excised and homogenized. CPT-11 and SN-38 were extracted using ice-cold acidic methanol and analyzed by HPLC methods, as reported previously.⁽⁵²⁾ The CPT-11 dose %/ml plasma or g tissue was calculated as the amount of CPT-11 per total plasma volume (ml) or per total tissue weight (g), respectively, from that of injected liposomal CPT-11.⁽⁵²⁾

2.7. Distribution of liposomal CPT-11 in TT xenograft mice

When the average tumor size reached approximately 150 mm^3 , mice were treated with Oct-CL or SL intravenously at a dose of 10 mg CPT-11/kg. At 6 h and 24 h after a single injection, tissues were collected and prepared as $20 \mu\text{m}$ frozen sections. Tissue sections were examined using an inverted microscope, ECRIPS TS100 (Nikon, Tokyo, Japan), with an Epi-Fluorescence Attachment (Nikon) a utilizing a UV1A filter.

2.8. Conversion activity of CPT-11 by carboxylesterase

The conversion activity of CPT-11 by carboxylesterase (CPT-CE activity) in TT cells, normal liver and TT tumor tissue was measured by the Guichard method.⁽⁶⁷⁾ Briefly, TT cells (4×10^4 cells) were homogenized. The

homogenates were centrifuged at 20,000 g for 30 min at 4°C to obtain cytosol.

Cytosolic protein (3 mg/ml, 80 µl) and 5 µM CPT-11 (20 µl) were mixed and incubated at 37°C for 1 h. Then, ice-cold acidic acetonitrile was added to stop the reaction. SN-38 produced during the incubation was measured by an HPLC method, as previously reported.⁽⁵²⁾ TT tumor tissue and liver were excised and homogenized. Cytosol from the TT tumor tissue and normal liver, which was perfused with ice-cold saline to remove blood, was prepared using the same protocol as for the extraction protocol in TT cells. CPT-CE activity in normal liver and TT tumor tissue was measured using the same protocol as for the assay protocol in TT cells.

2.9. Effects of octreotide-targeted liposomes on the PI3K/Akt/mTOR pathway in TT cells and TT tumors

TT cells were incubated with serum-starved (0.1% FBS) cell medium with empty Oct-CL, empty SL, CPT-11 or SN-38 for 24 h at 37°C. Cell lysates were prepared with ice-cold RIPA buffer (20 mM Tris-HCl (pH 7.5), 150 mM NaCl, 1% Triton X-100 containing protease and phosphatase inhibitors), separated by SDS-PAGE, and blotted using standard procedures.⁽⁶⁸⁾ Primary antibodies were against Akt, Tuberous sclerosis complex 2, tuberin (TSC2), p70S6K, phosphorylated Akt (Ser473), phosphorylated TSC2 (Thr1462) and phosphorylated p70S6K (Thr389) (all made in rabbits; Cell Signaling Technology, Beverly, MA, USA). Horseradish peroxidase-conjugated secondary antibody was used to detect the primary rabbit antibody (Santa Cruz Biotechnology, Inc., Santa Cruz, CA, USA). All proteins were detected by peroxidase-induced chemiluminescence (Super Signal West Pico Chemiluminescent substrate, Pierce).

When the average tumor size reached approximately 150 mm³, empty Oct-CL or empty SL was injected intravenously once (23.5 mg lipid and 867 nmol Oct/kg). At 24 h after injection, tumor tissue was collected and homogenized in RIPA buffer. Western blotting was performed using the same protocol as for the *in vitro* study.

2.10. Statistical analysis

The statistical significance of differences in the data was evaluated by

analysis using one-way ANOVA in combination with the Tukey-Kramer test. * $P < 0.05$ and ** $P < 0.01$ were considered as significant. Kaplan–Meier analysis was performed using GraphPad Prism, version 4.0, (GraphPad Software Inc. San Diego, CA).

3. Results

3.1 Size and zeta-potential of liposomes

Two types of liposomes, 1.6 mol% Oct-PEG-DSPE modified Oct-CL and 1.6 mol% PEG-DSPE modified SL were prepared. The average particle size of each liposome was ~146 nm with a narrow monodisperse distribution (data not shown). The zeta-potential and drug entrapment efficiency of each liposome formulation was approximately -14 mV and >80%, respectively (data not shown). There were no significant differences between Oct-CL and SL in terms of particle characters such as particle size, zeta-potential or drug entrapment efficiency, except for active-targeting ability.

3.2. Therapeutic efficacy of liposomal CPT-11

At first, the antitumor effect of free CPT-11, CL and Oct-CL were evaluated in TT xenografts. Oct-CL reduced the tumor size in mice after the final injections, and the reduced tumor size was maintained until the day 23 after the treatment, whereas CL maintained tumor growth suppression only until at day 10 after the treatment. Oct-CL suppressed tumor growth significantly compared with CL, free CPT-11 or saline (Fig. 12). Body weight losses were not observed in any of the groups (data not shown). Median survival for mice treated with saline was 68 days, compared with 88 days for free CPT-11-treated, 103 days for CL-treated mice and 217 days for Oct-CL-treated mice. Treatment with liposomal CPT-11 (CL and Oct-CL) significantly increased survival time. %ILS of Oct-CL-treated group (221.5) was significantly improved compared with that of the CL-treated (52.6) and free CPT-11-treated (30.4) groups.

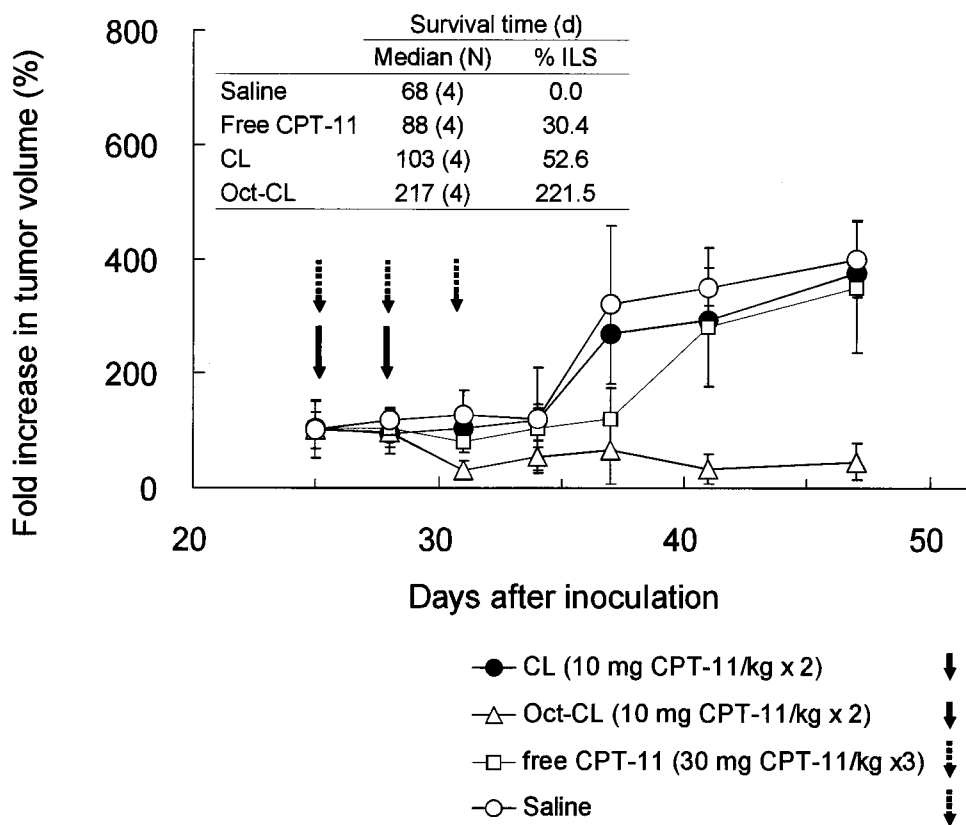


Figure 12. Effect of Oct-modification of liposomal CPT-11 on antitumor activity in mice bearing TT cells

Antitumor activity of Oct-CL was compared to that of CL or free drug. Liposomal CPT-11 (Δ : 10 mg/kg Oct-CL, \bullet : 10 mg/kg CL) was injected on days 24 and 27, and free CPT-11 (\square : 30 mg/kg) and saline (\circ) were injected three times. Arrows indicate the day of drug injections.

Each value represents the mean \pm S.D. (n = 4).

* Differences are statistically significant from free CPT-11 at $P < 0.05$.

Next, the antitumor effect of Oct-CL was compared with SL in TT tumor xenografts. Oct-CL exhibited significantly stronger suppression of tumor growth at day 31 to 52 after the inoculation compared with saline and at day 31 to 39 compared with SL (Fig. 13A). Body weights losses were not observed (Fig. 13B). Oct-CL treatment significantly improved median survival up to 212 days, compared with 198 and 121 days observed in SL-treated group ($P < 0.01$) and saline-treated group ($P < 0.05$), respectively (Fig. 13C).

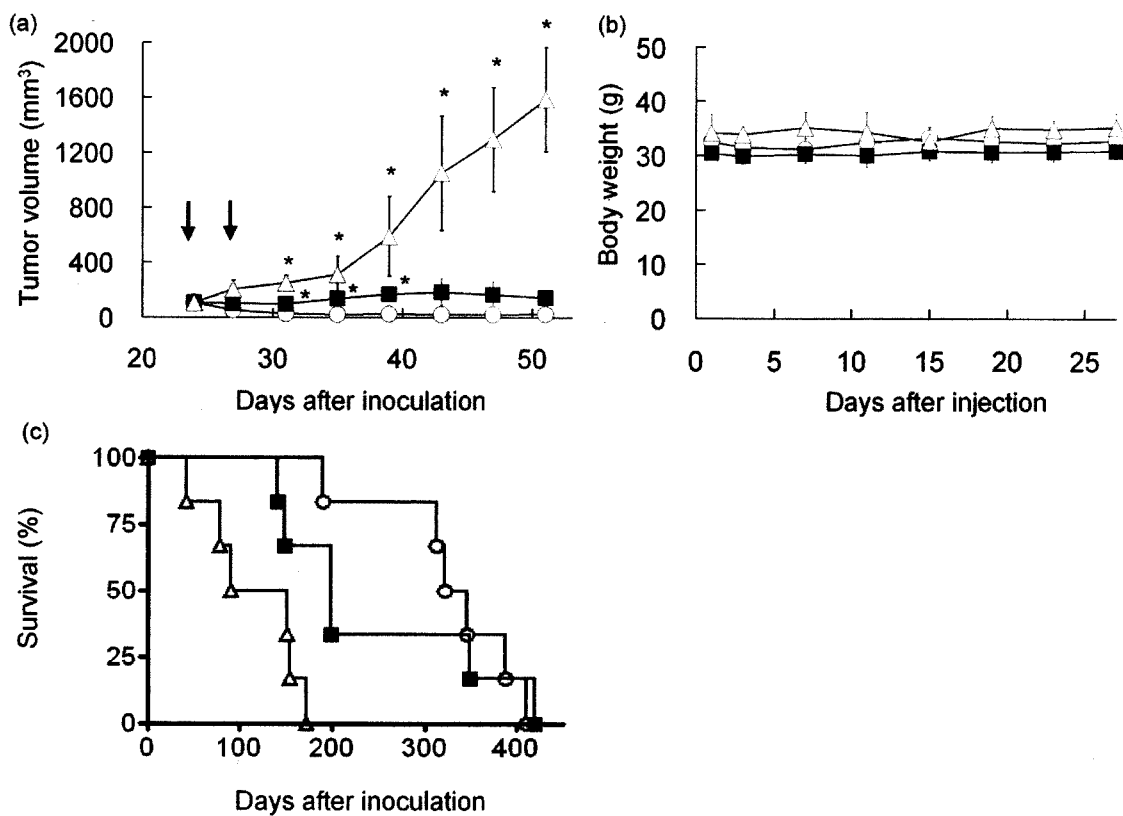


Figure 13. Therapeutic efficacy of administration of Oct-CL or SL. Oct-CL, SL or saline, was injected intravenously into mice. Treatment effects of liposomal CPT-11 on tumor size (A), body weight (B), and survival rate (C). The formulations used were Oct-CL (○), SL (■) and saline (Δ). Each value represents the mean \pm S.D. (n = 6). * $P < 0.05$ versus Oct-CL-treated mice.

3.3. Biodistribution of liposomal CPT-11

The biodistribution of CPT-11 and SN-38 was examined in TT xenografts at 6 h or 24 h after intravenous injections of Oct-CL or SL loaded with CPT-11. CPT-11 was highly distributed in the liver and spleen (Fig. 14B). Frozen sections of tumors in Oct-CL treated group were observed with blue fluorescence of CPT-11 than those in SL treated group, both 6 h and 24 h after injection (Fig. 14A). SN-38 could not be detected under this condition. CPT-11 blue fluorescence was weak and was not enough to show the significant difference in CPT-11 tumor accumulation between Oct-CL- and SL-treated groups. Therefore, next I measured concentrations of CPT-11 and SN-38 in tumor tissues and other organs by HPLC method. Six hours after

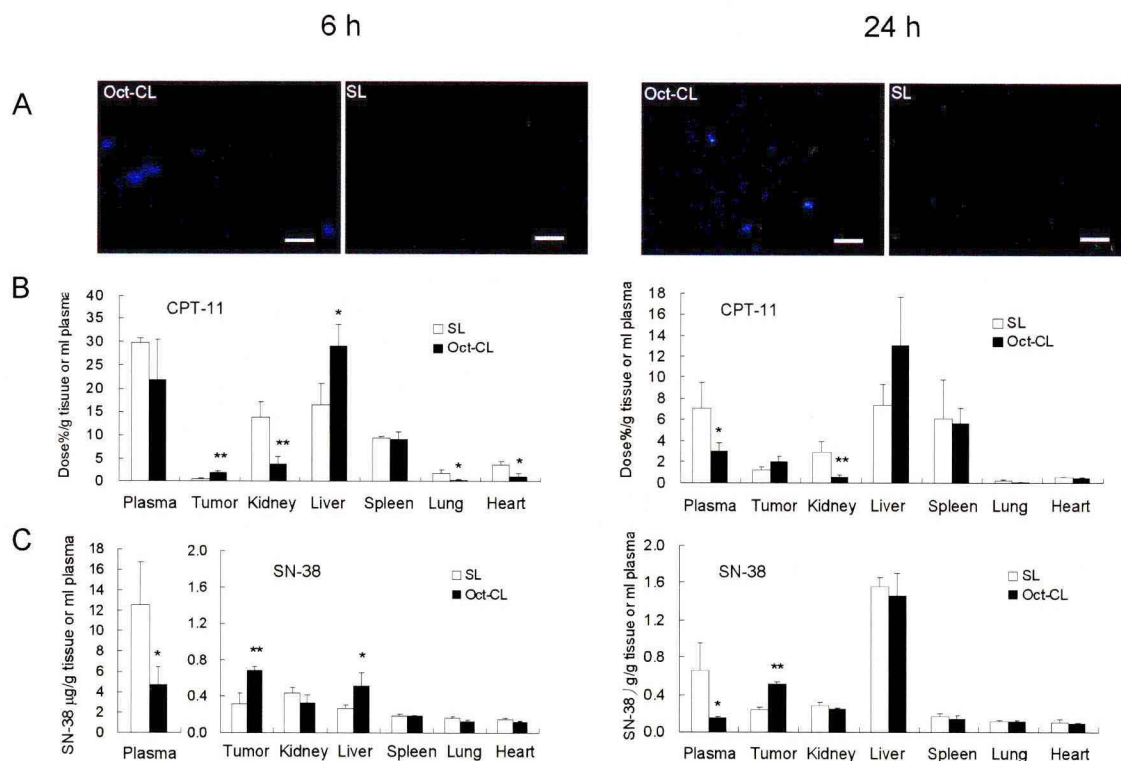


Figure 14. Biodistribution of liposomal CPT-11 at 6 h or 24 h after a single injection into mice

Frozen sections of tumors were observed using a fluorescence microscope (A), tissues biodistribution of CPT-11 (B), and SN-38 (C).

Each value represents the mean \pm S.D. (n = 3). * $P < 0.05$, and ** $P < 0.01$ versus SL.

Blue fluorescence; CPT-11. Scale bars; 100 μ m.

injection, CPT-11 levels in the liver of Oct-CL-treated mice were significantly higher than that of SL-treated mice ($P < 0.05$) (Fig. 14B and C). CPT-11 and SN-38 levels in tumor tissue of Oct-CL-treated mice were significantly higher, 3.7-fold and 2-fold, respectively, than compared with that of SL-treated mice ($P < 0.01$) (Fig. 14B and C). On the other hand, the kidney distribution of CPT-11 in Oct-CL-treated mice was significantly lower than that of SL-treated mice ($P < 0.01$). Twenty-four hours after injection, SL-treated mice maintained a higher CPT-11 level in the plasma ($7.1 \pm 2.4\%$ dose/ml), whereas Oct-CL-treated mice showed approximately half the CPT-11 plasma concentration of SL-treated mice ($P < 0.05$). Tumor CPT-11 concentration between the Oct-CL- and SL-treated groups was not significantly different, but the SN-38 concentration in Oct-CL-treated group was significantly higher, 2.2-fold, than in SL-treated mice ($P < 0.01$).

3.4. *In vitro* conversion of CPT-11 to SN-38 in TT cells, the liver and TT tumor tissues

In the biodistribution study, higher SN-38 accumulation was observed in tumor tissues 6 h and 24 h after administration of Oct-CL than that of SL. To confirm the conversion of CPT-11 to SN-38 in TT cells, I analyzed the *in vitro* conversion of CPT-11 to SN-38 in TT cells. The cytosol of TT cells showed the conversion of CPT-11 to SN-38 at a rate of 2.53 ± 0.09 pmol/h/mg protein (data not shown). TT cells *per se* were found to have the conversion activity of CPT-11 to SN-38. With regard to TT tumor tissue, the conversion rate in the liver was approximately 8.5% of the CPT-11 that was initially added to the reaction mixture (100 pmol CPT-11) (Fig. 15). Interestingly, the conversion of CPT-11 to SN-38 activity in TT tumor tissue was 0.8-fold that of the liver, suggesting that CPT-11 loaded into Oct-CL was accumulated in the tumor directly by active targeting of Oct-CL, and was converted into SN-38. The negative control (initially adding the stop solution before the addition of CPT-11 and incubation) showed no production of SN-38.

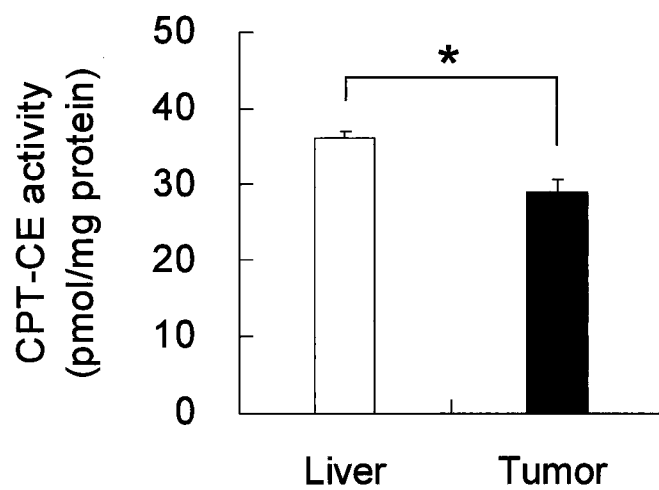


Figure 15. CPT-11 converted by carboxylesterase activity
Cytosol was incubated with CPT-11 at 37°C for 1 h.
Each value represents the mean \pm S.D. (n = 3). * $P < 0.05$.

3.5. Effects of Oct ligand of liposomes on growth inhibition and the phosphorylation of p70S6K

As shown in Fig. 16A, empty Oct-CL exerted growth inhibitory effect on TT cells in a dose-dependent fashion of Oct ligand. Furthermore, addition of 1.5 μM CPT-11 potentiated the growth inhibition activity of empty Oct-CL, having led to an additional approximately 20% of reduction in cell viability. In contrast, empty SL did not exert growth inhibitory effect in the presence or absence of CPT-11 (Fig. 16B). Free Oct showed growth inhibitory effect only at high-concentration, 100 μM (Fig. 16C), but showed no synergistic effect with CPT-11.

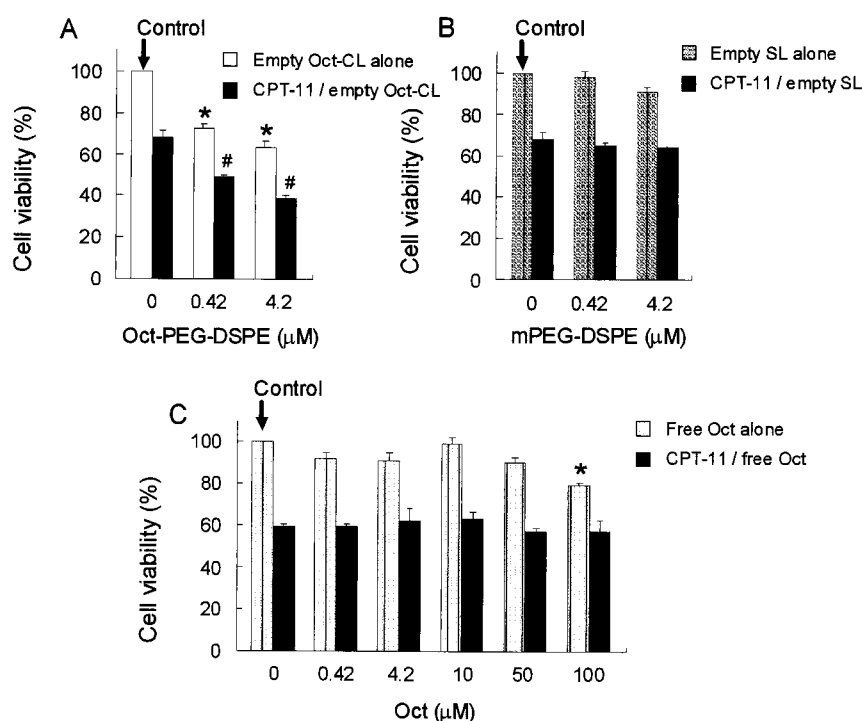


Figure 16. Cytotoxicity of free Oct or empty liposomes on TT cells in the presence or absence of 1.5 μM CPT-11

TT cells were treated with empty Oct-CL (A), empty SL (B) and free Oct (C), alone or combined with CPT-11. Each value represents the mean \pm S.D. (n = 4).

* $P < 0.05$ versus "Control" (cell viability of un-treatment).

$P < 0.05$ versus CPT-11 alone.

In many cancers, the PI3K/Akt/mTOR/p70S6K pathway contributes to cell proliferation and growth, and this pathway is activated by phosphorylation of Akt, TSC2 or p70S6K proteins.⁽⁷⁰⁾⁽⁷¹⁾ Therefore, I tried to clarify the effects of Oct ligand on phosphorylation of proteins in TT cells and TT tumors by Western blotting, using empty Oct-CL, empty SL, CPT-11 or SN-38. As shown in Fig. 17A, empty SL and empty Oct-CL did not affect the protein phosphorylation of neither Akt nor TSC2 in TT cells. Only empty Oct-CL (correspond to 0.42 μ M Oct ligand) strongly inhibited the phosphorylation of p70S6K at the Thr389 site whereas total p70S6K was not affected. In TT tumor tissue, whereas empty Oct-CL or empty SL did not affect total protein p70S6K, mice injected with empty Oct-CL showed a decrease in the level of phosphorylated p70S6K, but those with empty SL did not (Fig. 17B). However, the empty Oct-CL and the empty SL did not exhibit antitumor effects under this experiment condition in TT tumor xenografts (Fig. 18).

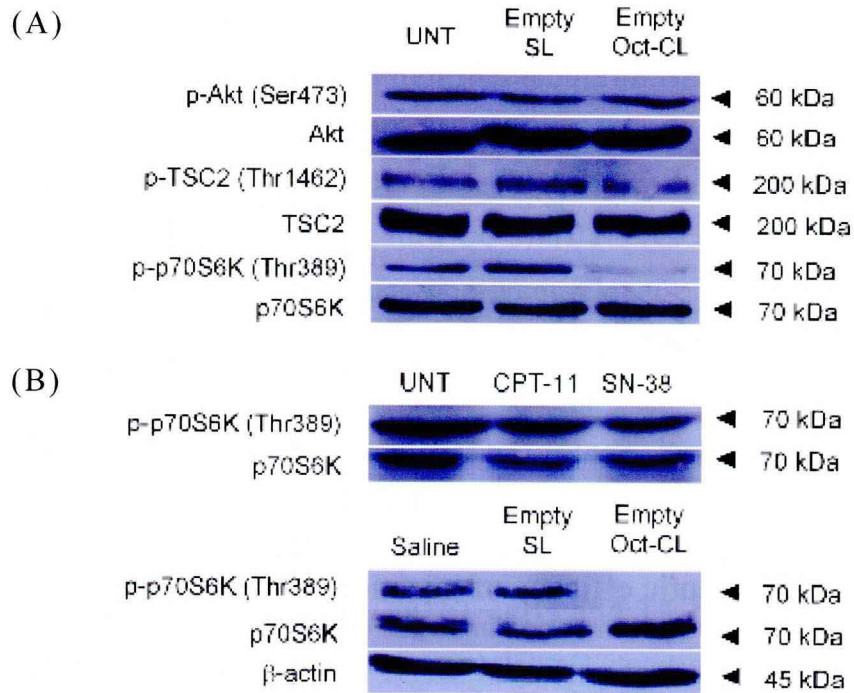


Figure 17. Effects of empty SL or empty Oct-CL on Akt-TSC2-p70S6K in TT cells (A) and TT tumor tissue (B)

TT cells were treated with empty Oct-CL (correspond to 0.42 μ M of Oct-PEG-DSPE), empty SL liposomes modified with 0.42 μ M PEG-DSPE, CPT-11 (13 μ M) or SN-38 (0.14 μ M) for 24 h. TT tumor-bearing mice were injected with empty Oct-CL 24 h before the experiment.

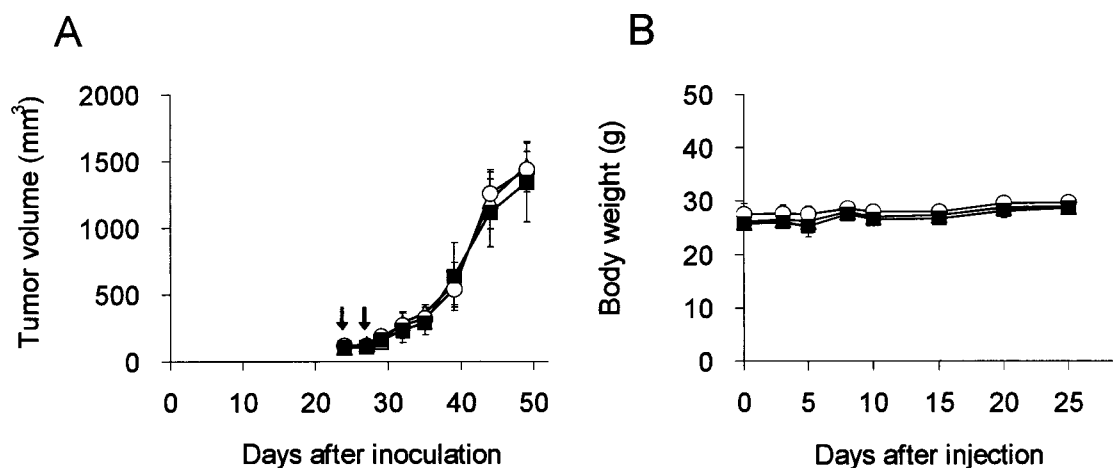


Figure 18. Therapeutic efficacy of injection of empty Oct-CL or empty SL. Treatment effects of empty liposomes on tumor size (A), body weight (B). The formulations used were empty Oct-CL (○), empty SL (■) and saline (Δ). Each value represents the mean \pm S.D. (n = 6).

4. Discussion

In this chapter, I demonstrated that Oct-CL showed the early and higher accumulation of CPT-11 in the tumor, enhanced the anti-tumor effect, and significantly prolonged the median survival compared with free CPT-11, CL and SL. Moreover, the mechanism of action of Oct associated with liposomes was investigated by measuring the biodistribution of Oct-CL and the phosphorylation of proteins after empty Oct-CL treatment.

In this Chapter, Oct-CL showed a significantly higher distribution to TT tumor tissue compared with SL at least until 6 h after injection. This result suggested that Oct-CL accumulated rapidly in the tumor after injection as a result of Oct-targeting, whereas SL accumulated slowly in the tumor by the EPR effect for 24 h. Twenty-four hour after injection, there was no significant difference in CPT-11 tumor accumulation between Oct-CL and SL. CPT-11 level of Oct-CL in the tumor was sustained for 24 h after injection.

Why was the SN-38 concentration of tumors in Oct-CL-treated mice significantly higher than that of SL-treated mice at 24 h even though the CPT-11 concentration was similar? Generally, it is reported that CPT-11

conversion to SN-38 mainly occurs through the action of liver carboxyl esterase.⁽⁶⁷⁾ Accordingly, it can be regarded that SN-38 transformed in the liver accumulated in the tumor. When the accumulation of CPT-11 in the liver was similar between Oct-CL- and SL-treated mice, converted SN-38 in the liver should be present in similar amounts, and, therefore, the amount of SN-38 accumulating in tumor should be similar. As described in Chapter 1, there were no significant differences between Oct-CL and SL in terms of drug release over 48 h at 37°C in PBS. Furthermore, an *in vitro* conversion study showed that the conversion activity of CPT-11 to SN-38 in TT tumor tissue was 0.8-fold that of the liver. From these findings, higher SN-38 concentration of Oct-CL at 24 h may reflect early direct distribution of Oct-CL to tumor tissue by SSTR-targeting. To the best of our knowledge, this is first report about CPT-11 conversion activity in TT cells and TT tumor tissue.

When I examined other tissues, there were significant differences between Oct-CL- and SL-treated mice in kidneys and liver distribution. The CPT-11 concentration in the kidneys of Oct-CL-treated mice was significantly lower compared with that of SL-treated mice. Because the kidney is known to express SSTR2,⁽⁶⁹⁾ Oct-CL might be selectively and rapidly distributed to the kidneys, as well as to the tumor, and then excreted more rapidly than in SL-treated mice. With regard to the liver, Oct-CL accumulated to a higher level in the liver than with SL because SL was modified with Oct ligand and it may be taken up by the RES.

Empty Oct-CL exerted cell growth inhibition at low-concentrations (0.42 and 4.2 μ M), while free Oct did not show it below 100 μ M (Fig. 15). Empty Oct-CL showed effectively cell growth inhibition compared with free Oct, suggesting that affinity of empty Oct-CL to SSTR may be higher than that of free Oct. Phosphorylation of p70S6K is reported to activate cell growth and proliferation.⁽⁷⁰⁾ p70S6K is the downstream protein of the PI3K/Akt/mTOR pathway (Fig. 19) and phosphorylation of p70S6K is generally used as a marker of the inhibition of the PI3K/Akt/mTOR/p70S6K pathway.⁽⁷¹⁾ Treatment with empty Oct-CL caused the suppression of phosphorylation of p70S6K *in vitro* and *in vivo* (Fig. 17) but empty SL did not. Therefore, this result suggested that empty Oct-CL inhibited cell growth and proliferation by suppressing the phosphorylation of p70S6K in TT cells and TT tumor tissue. In other words, the targeting-ligand Oct had not only tumor

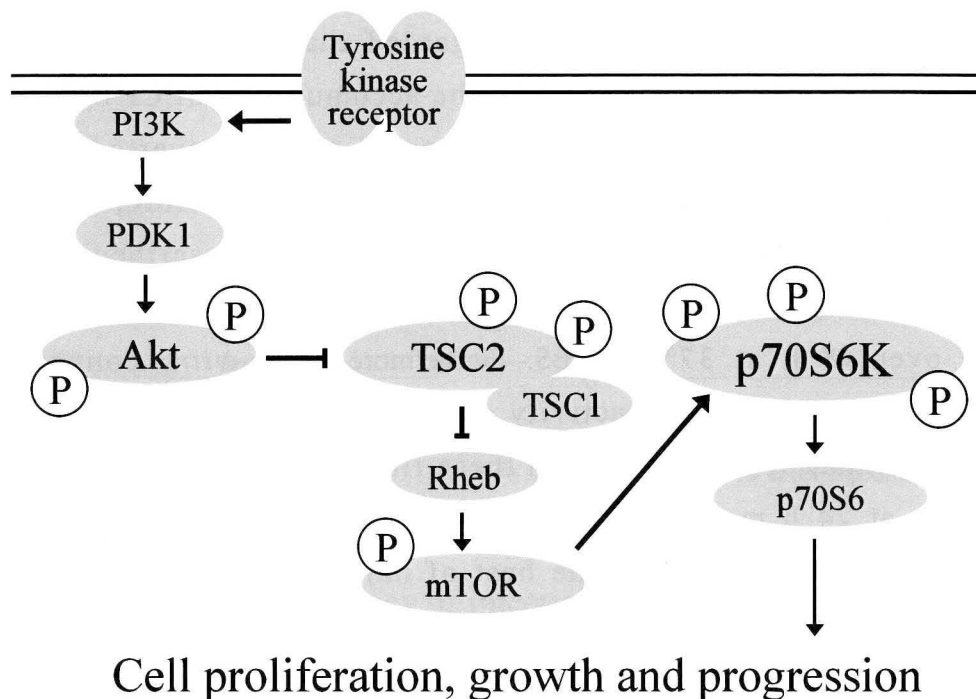


Figure 19. The PI3K/Akt/mTOR pathway in insulinoma cell line

targeting activity but also assisted with the antitumor effects. Therefore, the Oct ligand has dual functionality.

However, the treatment with empty Oct-CL did not exhibit anti-tumor effect under this condition (Fig. 18). For MTC, it was reported that clinically subcutaneous injection of free Oct at 500 μg (= 458 nmol)/day for 90 days, and 150 μg (= 137 nmol)/day for 6 months showed no effects to therapeutic efficacy.^(59, 60) In this therapeutic study, Oct originated from Oct-CL was injected twice as 867 nmol Oct/kg/day. From these different schedules, it is difficult to judge the therapeutic efficacy by Oct alone in our study.

Fig. 20 illustrates the proposed antitumor effects of Oct-CL for MTC. Oct-CL was selectively associated with TT cells. CPT-11 was released from Oct-CL, and then CPT-11 was converted to SN-38 by carboxylesterase in TT tumor. SN-38 produced in the tumors showed cytotoxicity. Oct-CL suppressed the phosphorylation of p70S6K. These suppressions led to inhibition of cell growth and proliferation, which assisted in anti-tumor effects for MTC using Oct-CL loaded with CPT-11.

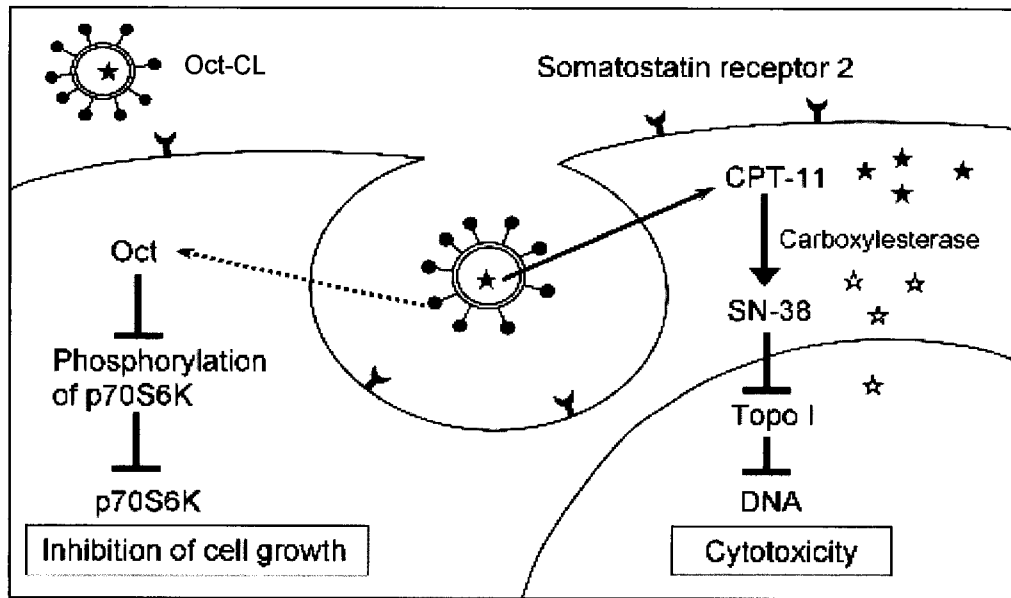


Figure 20. Proposed mechanisms of antitumor effects of Oct-CL for MTC

5. Conclusion

In Chapter 2, it was showed that Oct-CL exhibited enhanced drug accumulation in tumor, and CPT-11 in tumor was converted into an active metabolite 0.8-fold that in the liver. Oct-targeted liposome exhibited higher therapeutic efficacy with the strong antitumor effect and the significant improvement of median survival, than free CPT-11, non-PEGylated liposome, CL and PEGylated liposome, SL in TT tumor xenografts. Empty Oct-CL in TT cells and tumor decreased the level of phosphorylated p70S6K. The improvement in therapeutic efficacy was due to the dual functions of Oct; the rapid and highly selective distribution of Oct-CL to tumor by SSTR-targeting and the assistance of cell growth suppression by mTOR inhibition.

CHAPER 3

Liposomal everolimus for the treatment of lung carcinoma and medullary thyroid carcinoma *in vivo*

1. Introduction

As described in Chapter 2, empty Oct-targeted liposomes (empty Oct-CL) decreased the level of phosphorylated p70S6K in TT cells and tumors. Oct, a ligand of SSTR exhibited mTOR inhibition. However, empty Oct-CL did not show therapeutic efficacy to MTC *in vivo*.

Rapamycin interferes with the PI3K/Akt/mTOR/p70S6K signaling cascade, which activates cell growth and cell proliferation.^(70,71) Although rapamycin was discovered more than 30 years ago, renewed interest in this pathway is evident by the numerous rapamycin analogs (rapalogs) developed recently.⁽⁷²⁾ Some rapalogs have recently become of significant interest as potential anti-cancer drugs.⁽⁷³⁻⁷⁵⁾ Everolimus (Fig. 21) is a rapalog 40-*O*-(2-hydroxyethyl) derivative of rapamycin. Everolimus was approved as only anticancer agent based on an mTOR inhibition in Japan in 2009.

Two problematic features of rapamycin and rapalogs are their low water solubility (everolimus, 9.6 µg/ml) and low biological availability.^(76, 77) Therefore, to circumvent such unsuitable characteristics, rapamycin was entrapped in liposomes, polymer micells or albumin-bound nanoparticles.⁽⁷⁸⁻⁸⁰⁾ However, so far, to our best knowledge, there is no report of the antitumor efficacy *in vivo* of liposomal rapamycin or other particulated rapalogs.

Therefore, I examined the antitumor effect of liposomal everolimus as an mTOR inhibitor *in vitro* and *in vivo*. In addition, the cytotoxicity of co-administration of everolimus and CPT-11 was examined *in vitro*, to compare with the previous results of combination of empty Oct-CL and CPT-11.

In this Chapter, I examined the antitumor activity of a liposomal formulation of everolimus *in vitro* and *in vivo*.

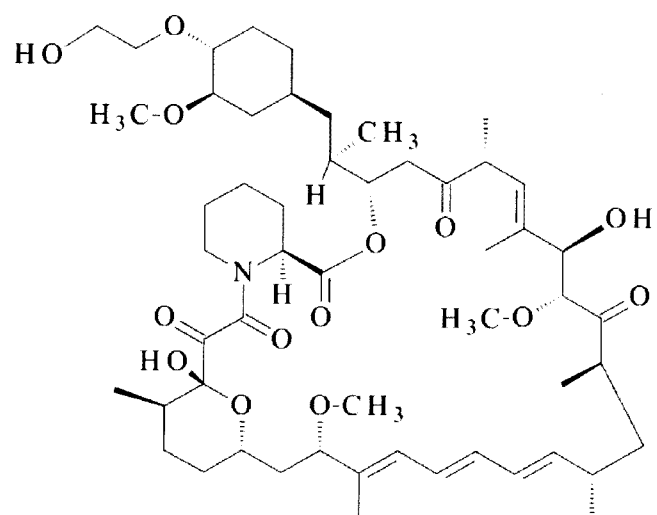


Figure 21. Chemical structure of everolimus

2. Experimental section

2.1. Materials

Everolimus was purchased from LC laboratories (Woburn, MS, USA). Soybean L-alpha-lecithin (soybean lecithin) was purchased from Calbiochem (Darmstadt, Germany). RPMI medium was purchased from Wako Pure Chemical Industries, Ltd. (Osaka, Japan). CPT-11, DSPC, mPEG-DSPE, Chol, Ham's F-12 medium and FBS were the same ones described in Experimental section of Chapter 1 and 2. Other reagents were analytical or HPLC grade.

2.2. Cell cultures and cell preparations

Culture of TT cells was described in Experimental section of Chapter 1. Human-derived small cell lung carcinoma NCI-H446 and breast cancer MCH-7 were from American Type Cellular Collection (ATCC, Manassas, VA, USA). NCI-H446 cells and MCF-7 cells were maintained in RPMI medium. The medium was supplemented with 10% heat-inactivated FBS at 37°C in a humidified atmosphere containing 5% CO₂.

2.3. Preparation of liposomal everolimus

Four kinds of liposomal everolimus were prepared. The liposome compositions by molar ratio were DSPC/Chol/PEG-DSPE (52:42:6, D-SL), DSPC/Chol (55:45, D-CL), soybean lecithin/Chol/PEG-DSPE (89:5:6, S-SL) and soybean lecithin/Chol (95:5, S-CL). Liposomes composed with DSPC or soybean lecithin are indicated with D or S, respectively. PEGylated liposomes and non-PEGylated liposomes are indicated as SL and CL, respectively. Therefore, D-SL indicates PEGylated liposomes composed of DSPC and Chol (Table 5). Liposomal everolimus was prepared by an ethanol injection method.⁽⁸¹⁾ Briefly, all lipids (20 mg) and everolimus were dissolved in ethanol (2 ml). This alcoholic solution was added into distilled water (4 ml) immediately, followed by sonication to decrease the size of liposomes to approximate 100 nm. The residual ethanol was removed by evaporation under reduced pressure. The resulting mean diameter of the liposomes was measured by dynamic light scattering (ELS-Z2, Otsuka Electronics, Osaka, Japan) at 25°C after diluting the liposome suspension with water. The entrapment efficiency of everolimus was calculated by separating un-encapsulated from encapsulated drug by gel filtration chromatography using a Sephadex G50

column. The everolimus concentration was measured with the use of an HPLC system (Shimadzu Co., Kyoto, Japan) composed of an LC-20AT pump, an SIL-20A autoinjector and an SPD-M20A detector measuring absorbance of 278 nm, using a TSKgelODS-80Ts QA 5 mm column (4.6 mm I.D. x 250 mm, TOSHO, Co., Ltd., Tokyo, Japan). The mobile phase was 20% methanol at a flow rate of 1 ml/min. Under these conditions, everolimus was eluted at 10.1 min. The everolimus concentration of each sample was determined using a calibration curve. The everolimus-to-lipid molar ratio was 0.02, as referenced from a previous report,⁽⁷⁹⁾ and the final lipid concentration was approximately 1 mg/ml.

2.4. Cytotoxicity assay

Cells were seeded into 96-well plates at a density of 10^4 cells/well for 24 h before addition of the drug. Culture medium was replaced with fresh medium, containing various concentrations of free everolimus. After 48 h incubation with free and liposomal everolimus at 37°C, the cells were washed with PBS three times. Then, cell viability was determined using a WST-8 test (Dojindo Laboratories, Kumamoto, Japan). All measurements were carried out in quadruplicate. IC₅₀ was calculated using the bootstrap method.⁽⁵⁴⁾

To evaluate co-treatment cytotoxicity of free everolimus and CPT-11 on these cells, cells were incubated with 10-100 nM everolimus in the absence or presence of 1.5 μ M CPT-11 for 48 h at 37°C.⁽⁸²⁾ Cell viability was determined as described above.

2.5. Animal experiments

All animal experiments were performed with approval from the Institutional Animal Care and Use Committee at Hoshi University. NCI-H446 cells (1×10^7) were inoculated subcutaneously into female BALB/c nu/nu mice (6 weeks of age, CLEA Japan, Inc., Tokyo, Japan). When the average tumor volume was approximately 100 mm³, free everolimus was administrated intraperitoneally at a dose of 1 mg or 5 mg/kg, in five injections at five-day intervals. Free everolimus was unable to be injected intravenously because of low solubility in water. Therefore, everolimus solution in mixture of 5% polyethylene glycol and 5% Tween-80, was intraperitoneally injected. D-SL was administrated intravenously equivalent to 5 mg everolimus/kg. Tumor volume and body

weight were measured as described in Experimental section of Chapter 2

2.6. Statistical analysis

It was described in 2.10 of Chapter 2.

3. Results

3.1. Size and zeta-potential of liposomes

Table 5 presents the particle size and everolimus entrapment efficiency of liposomal formulations. The results indicated that all liposome sizes were ~80 nm with a polydispersity less than 0.19. Entrapment efficacies of everolimus were very different between D-CL and S-CL. S-CL showed 95.7% entrapment efficiency, but the value for D-CL was 6.5%. Meanwhile, D-SL, PEGylated D-CL, showed an 88.4% entrapment efficiency. Therefore, liposomal everolimus in the forms of D-SL, S-SL and S-CL were used in the following experiment.

Table 5. Characteristic of liposomal everolimus

Formulation	Abbr.	Size (nm)	Polydispersity	Entrapment efficacy (%)
DSPC/Chol/PEG-DSPE	D-SL	76.1 ± 2.0	0.178 ± 0.017	88.4 ± 4.3
DSPC/Chol	D-CL	91.4 ± 23.9	0.169 ± 0.029	6.5 ± 1.5
Soybean lecithin /Chol/PEG-DSPE	S-SL	68.0 ± 5.5	0.161 ± 0.045	92.7 ± 5.7
Soybean lecithin /Chol	S-CL	77.9 ± 3.3	0.188 ± 0.013	95.7 ± 2.0

Note; Mean ± S.D. (n = 3).

3.2. Antitumor effect of liposomal everolimus *in vitro*

I chose three tumor cell lines to evaluate the cytotoxicity of free and liposomal everolimus. In MCF-7 cells and NCI-H446 cells, the PI3K/Akt/mTOR/p70S6K pathway was reported to be active, and mTOR pathway inhibition showed anticancer effects in an *in vitro* study.^(83, 84) MCF-7 cells and NCI-H446 cells were used as positive controls. TT cells were used to evaluate the cytotoxicity of octreotide-modified liposomes in Chapters 1 and 2.^(66, 85) The IC₅₀ values of free everolimus in NCI-H446 cells, TT cells and MCF-7 cells were 73.1 ± 25.3 nM, 153.4 ± 12.2 nM and more than 260 nM, respectively (Table 6). This finding indicated that the sensitivity of cytotoxicity of everolimus in these tumor cells was higher in this order; NCI-H446 > TT > MCF-7. Therefore, I selected NCI-H446 and TT cells for further experiments.

Table 6. Cytotoxicity of free everolimus

Cell line	IC50 (nM)
NCI-H446	73.1 ± 25.3
TT	153.4 ± 12.2
MCF-7	> 260

Note; Mean ± S.D. (n = 4).

Next, I examined the cytotoxicity of liposomal everolimus. As shown in Fig. 22, the IC50 of all liposomal everolimus formulations except for D-SL in NCI-H446 cells were over 260 nM after 48 h incubation, indicating that the cytotoxicity in liposomal everolimus was reduced compared with free everolimus. In liposomal everolimus, D-SL showed the highest cytotoxicity for both cell types, suggested that release of the drug from D-SL might occur during the 48 h incubation. From Table 6 and Fig. 22, I estimated that everolimus in D-SL may be kept in liposomal lipid outer membrane by PEG-lipid and may be released more easily than in S-CL or S-SL. Therefore, I selected D-SL for *in vivo* experiments.

3.3. Antitumor effect on NCI-H446 tumor xenografts

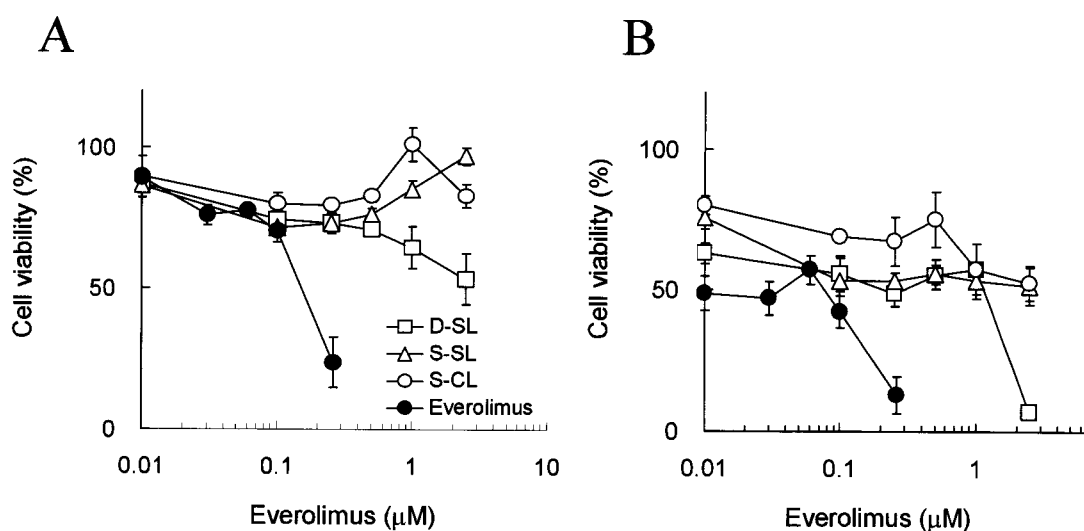


Figure 22. Cytotoxicity of liposomal everolimus in TT cells (A) or NCI-H446 cells (B)

Cells were incubated with liposomal everolimus at various concentrations for 48 h.

Each value represents the mean ± S.D. (n=4).

The antitumor activity of free and liposomal everolimus was evaluated after five injections as five-day intervals into NCI-H446 tumor xenografts. Tumor inoculation day was defined as day 0. As shown in Fig. 23A, one mg/kg-treated mice did not get significant tumor suppression compared with saline-treated mice by day 70. Free everolimus- or D-SL-treated mice, at a dose of 5 mg/kg, showed tumor suppression, compared with saline at day 39 to day 59 ($P < 0.05$). Body weight loss was not observed in any of the treatment groups (Fig. 23B).

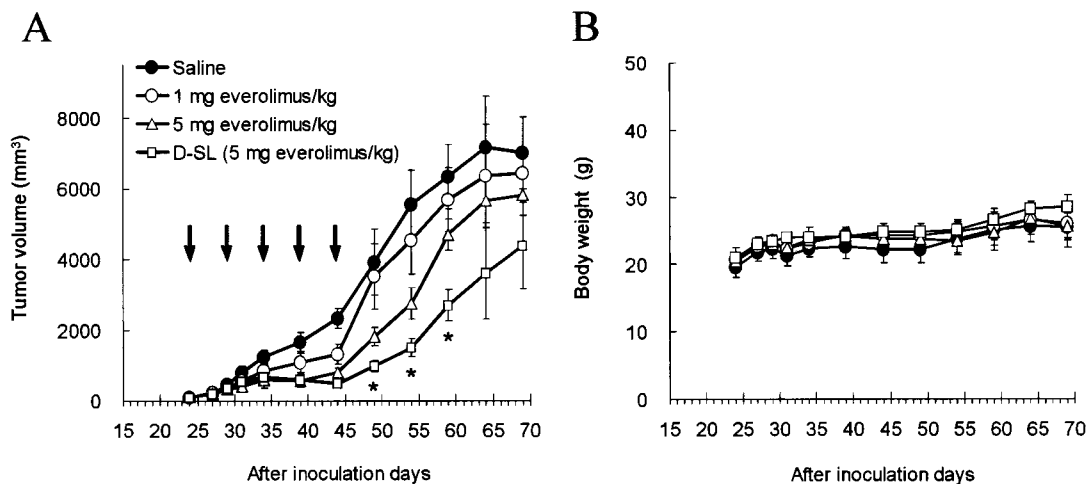


Figure 23. Effect of free and liposomal everolimus on antitumor activity (A) and body weight change (B) in mice bearing NCI-H446 tumors

Antitumor activity and toxicity were assessed by measuring tumor volume and body weight change after intraperitoneal injections of free everolimus and after intravenous injections of D-SL (equivalent to 5 mg everolimus/kg). D-SL (□), free 5 mg (Δ), free 1 mg everolimus/kg (○) or saline (●) were administrated on days 24, 29, 34, 39 and 44 days after inoculation, as shown by arrows.

Each value represents the mean \pm S.D. (n = 6).

*, Statistically significant differences between free 5 mg everolimus/kg and D-SL ($P < 0.05$).

3.4. Co-treatment efficacy with everolimus and CPT-11 *in vitro*

Everolimus was reported to have synergistic cytotoxicity in combination with other chemotherapeutic agents on several cancer cell types.⁽⁸¹⁻⁸³⁾ Moreover, I described that mTOR pathway inhibition by octreotide-modified liposome without drug loading enhanced cell cytotoxicity in the presence or absence of CPT-11 in TT cells in Chapter 2. Everolimus is an mTOR inhibitor, and octreotide-modified liposomes functioned as an mTOR inhibitor. Therefore, I compared the cytotoxicity of a combination of CPT-11 and everolimus with that of CPT-11 and octreotide-modified liposomes. Similar to my result in Chapter 2 of co-treatment of 1.5 μM CPT-11 and octreotide-modified liposomes, the cytotoxicity of everolimus in the absence or presence of CPT-11 increased in a dose-dependent manner for everolimus in all treatments of NCI-H446 cells (Fig. 24).

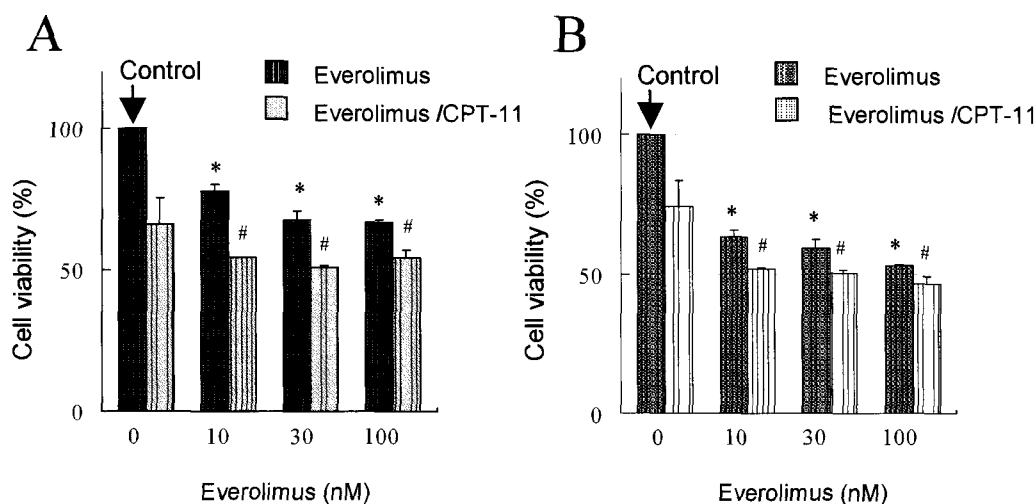


Figure 24. Co-treatment effects of free everolimus in the absence or presence of free CPT-11 on cell viability in TT cells (A) or NCI-H446 cells (B)

Cells were treated with 10-100 nM everolimus in the presence or absence of 1.5 μM CPT-11 for 48 h. The data represent the means \pm S.D. (n = 4).

*, Statistically significant differences between “control” (no treatment) and everolimus treatment ($P < 0.05$).

#, Statistically significant differences between CPT-11 alone and co-treatment with everolimus and CPT-11 ($P < 0.05$).

4. Discussion

In this Chapter, I prepared liposomal everolimus and demonstrated that a significant therapeutic efficacy with the liposomes *in vitro* and *in vivo*.

Regarding entrapment efficiency of liposomal everolimus, S-CL showed high entrapment efficiency, but the value for D-CL was low. This result for S-CL agreed with a previous report.⁽⁷⁹⁾ Soybean lecithin is composed of mainly linoleic acid (62-65%) with a double bond. Therefore I estimated that everolimus might interact with the double bond of linoleic acid.

Meanwhile, D-SL, PEGylated D-CL, showed more than 80% entrapment efficiency. With the increase in the PEG-DSPE ratio in the liposome composition, the entrapment efficiency of everolimus increased (data not shown). Thus, in the case of the liposomes consisting of DSPC, PEG-lipid may assist the entrapment of everolimus into the liposome membrane.

In therapeutic study in NCI-H446 xenografts, significant antitumor efficacy was observed. In a comparison with the free everolimus-treatment group, the liposomal everolimus-treatment group without body weight losses at a dose of 5 mg/kg showed significant tumor suppression at day 49 to day 59 ($P < 0.05$), which reflected the prolongation of drug activity with the use of a liposomal formulation. To the best of our knowledge, this is the first report of the anti-tumor efficacy of liposomal everolimus in an *in vivo* experiment. It was reported that one of the features of rapalog is lifespan extension.⁽⁸⁶⁾ With regard to the survival, two saline-treated mice died during 97 days period of the study, and both had large tumors (approximately 10^5 mm^3) (data not shown). Although free or liposomal everolimus-treated mice also bore large-tumors, all of the mice were alive at the end of the 97 day study period. Median survival for mice treated with saline was 125.5 days, compared with 136 days for 1 mg everolimus-treated, 137 days for 5 mg everolimus-treated, and 146 days for D-SL (5 mg everolimus/kg)-treated mice. The %ILS value of 1 mg everolimus/kg-treated, 5 mg everolimus/kg-treated and D-SL (5 mg everolimus/kg)-treated mice was 8.4, 9.2 and 16.3, respectively. There is a significant difference tendency between the survival time of D-SL-treated mice and that of saline-treated mice ($P = 0.055$ by log-rank test). In this study, lifespan was also evaluated to be increased in liposomal everolimus.

Moreover, mTOR inhibition effect in NCI-H446 cells by everolimus showed significant antitumor effects in the presence and absence of CPT-11, at everolimus dose-dependent manner. Therefore, in the future, if the dose of everolimus and CPT-11 in combination therapy was optimized, efficient therapeutic efficacy should be achieved in an *in vivo* experiment.

5. Conclusion

In conclusion, I was able to prepare liposomal everolimus and succeeded the TT tumor cell growth-suppression *in vitro*, and the NCI-H446 tumor-suppression *in vitro* and *in vivo*, using this formulation of mTOR inhibitor.

SUMMARY

Developing new approaches toward rare cancers are very important from a social and medical viewpoint. Furthermore, efforts to generate therapies for rare cancers might clarify new viewpoints and provide insight into the treatment of common cancers. MTC, one of the rare cancers has been lacking in effective therapeutic treatment except for surgery. In animal study, therapeutic efficacy for MTC using CPT-11 has been reported. However, the approach was fail as consequence of serious side effects. To increase the therapeutic efficacy of MTC with CPT-11, it is necessary of active-targeting, selective delivery of drug to tumor sites. For this purpose, particulate drug carriers are useful. Especially, particle surface modification with tumor targeting ligand is a promising method to high therapeutic efficacy. However, when targeting moieties are employed to liposomes, their circulation times are often decreased *in vivo*, owing to recognition by the RES. Thus, it is difficult to generate active targeting liposomes for cancer therapy.

In this thesis, Oct-targeted liposomes loaded with CPT-11 were prepared, evaluated and compared with free CPT-11, non-PEGylated liposomes and PEGylated non-targeted liposomes for MTC therapy. Moreover, the functions of Oct ligand were clarified.

In Chapter 1, it was demonstrated that Oct-targeted liposomes loaded with CPT-11 associated selectively with TT cells *via* somatostatin receptor. Optimal Oct-modification of liposomes for cellular uptake was more than 1.4mol%. Thus, 1.6mol% Oct-targeted liposomes loaded with CPT-11 may be able to offer a high therapeutic potential for MTC. In addition, it was observed that 20% cell death in TT cells was caused by 100 μ M free Oct and 0.42 μ M Oct ligand. Thus, I found that empty Oct-targeted liposomes exhibited 238-fold higher cytotoxicity than free Oct in TT cells.

In Chapter 2, Oct-targeted liposome exhibited MTC therapeutic efficacy *in vivo*: strong antitumor effects and the lifespan-expansion, compared with free CPT-11, non-PEGylated liposomes and PEGylated liposomes. Moreover, from the results of the biodistribution and bioconversion of Oct-targeted liposomes, it was demonstrated that Oct ligands delivered selectively the liposomes to tumor sites, and the released

CPT-11 in tumor may be converted into active metabolite, SN-38. From Chapters 1 and 2, it was clarified that Oct-targeted liposomes loaded with CPT-11 are effective for MTC therapy, due to the selective delivery of drug and the assistance of cell growth suppression by Oct-ligand. Oct-ligand, empty Oct-targeted liposomes, inhibited PI3K/Akt/mTOR pathway. However, empty Oct-targeted liposomes did not show antitumor effect *in vivo*, suggesting that contributing to prolong the time to tumor progression. Thus, I examined antitumor effect of mTOR inhibitors *in vivo* as an active control.

In many cancer cells including MTC cells, lung cancer cells, and breast cancer cells and so on, PI3K/Akt/mTOR pathway is activated to cell growth and cell proliferation. Everolimus was selected as a model drug of an mTOR inhibitor. In Chapter 3, liposomal everolimus was prepared to evaluate the antitumor effect of an mTOR inhibitor in MTC cells and lung cancer cells. The liposome formulation of everolimus was able to suppress the tumor growth of both cells. Therefore, liposomal mTOR inhibitor affords the possibility of different formulations to treat MTC.

In conclusion, active targeting, Oct-targeted liposomes loaded with CPT-11 will be useful for treatment of MTC. Oct-targeted liposomes exhibited that Oct ligand is effectively recognized by somatostatin receptors and acts tumor cell growth suppression *via* mTOR inhibition more than free Oct. Oct-targeted liposomes will be one of effective formulations for Oct, single drug when binding with somatostatin receptors and/or high concentration in targeted cells are needed. Furthermore, in dual-targeted approach therapy with Oct, Oct-targeted liposomes will provide one particle formulation if another drug can be loaded in the same particles. Oct-targeted particles may give further opportunities to treatments of not only MTC, rare cancers, but also somatostatin receptor positive- and PI3K/Akt/mTOR pathway activated-tumors, such as lung carcinoma, common cancers.

ACKNOWLEDGEMENTS

This research will never be materialized without the help of the following people:

First, I would like to express my gratitude and appreciation to Professor Yoshie Maitani for helpful guidance in my research work and preparing this dissertation.

Further, I wish to thank Professor Hiraku Onishi and Professor Tsutomu Tsuji for their valuable assistance in my research work.

Also I would like to thank Associate Professor Yoshiyuki Hattori and Dr. Kumi Kawano for their helpful assistance in my research work.

Moreover, Also I would like to thank Dr. Teruaki Oku (Department of Microbiology, Hoshi University) for his helpful assistance in my research work.

In addition, I would like to thank the members of Fine Drug Targeting Research Laboratory for their friendship and assistance.

Finally, I will be forever in debt to my family for their support, words and comprehensions.

REFERENCES

1. Vitale G, Caraglia M, Ciccarelli A, Lupoli G, Abbruzzese A, Tagliaferri P. Current approaches and perspectives in the therapy of medullary thyroid carcinoma. *Cancer*. 2001;91:1797-808.
2. Cakir M, Grossman AB. Medullary thyroid cancer: molecular biology and novel molecular therapies. *Neuroendocrinology*. 2009;90:323-48.
3. Giuffrida D, Gharib H. Current diagnosis and management of medullary thyroid carcinoma. *Ann Oncol*. 1998;9:695-701.
4. Wells SA, Robinson BG, Gagel RF, Dralle H, Fagin JA, Santoro M, et al. Vandetanib in Patients With Locally Advanced or Metastatic Medullary Thyroid Cancer: A Randomized, Double-Blind Phase III Trial. *J Clin Oncol*. 2011.
5. Strock CJ, Park JI, Rosen DM, Ruggeri B, Denmeade SR, Ball DW, et al. Activity of irinotecan and the tyrosine kinase inhibitor CEP-751 in medullary thyroid cancer. *J Clin Endocrinol Metab*. 2006;91:79-84.
6. Koga K, Hattori Y, Komori M, Narishima R, Yamasaki M, Hakoshima M, et al. Combination of RET siRNA and irinotecan inhibited the growth of medullary thyroid carcinoma TT cells and xenografts via apoptosis. *Cancer Sci*. 2010.
7. Kawato Y, Furuta T, Aonuma M, Yasuoka M, Yokokura T, Matsumoto K. Antitumor activity of a camptothecin derivative, CPT-11, against human tumor xenografts in nude mice. *Cancer Chemother Pharmacol*. 1991;28:192-8.
8. Kawato Y, Aonuma M, Hirota Y, Kuga H, Sato K. Intracellular roles of SN-38, a metabolite of the camptothecin derivative CPT-11, in the antitumor effect of CPT-11. *Cancer Res*. 1991;51:4187-91.
9. Hsiang YH, Wu HY, Liu LF. Topoisomerases: novel therapeutic targets in cancer chemotherapy. *Biochem Pharmacol*. 1988;37:1801-2.
10. Hsiang YH, Liu LF, Wall ME, Wani MC, Nicholas AW, Manikumar G, et al. DNA topoisomerase I-mediated DNA cleavage and cytotoxicity of camptothecin analogues. *Cancer Res*. 1989;49:4385-9.
11. Hsiang YH, Lihou MG, Liu LF. Arrest of replication forks by drug-stabilized topoisomerase I-DNA cleavable complexes as a mechanism of cell killing by camptothecin. *Cancer Res*. 1989;49:5077-82.

12. Ohno R, Okada K, Masaoka T, Kuramoto A, Arima T, Yoshida Y, et al. An early phase II study of CPT-11: a new derivative of camptothecin, for the treatment of leukemia and lymphoma. *J Clin Oncol.* 1990;8:1907-12.
13. Nakanishi T, Fukushima S, Okamoto K, Suzuki M, Matsumura Y, Yokoyama M, et al. Development of the polymer micelle carrier system for doxorubicin. *J Control Release.* 2001;74:295-302.
14. Yoo HS, Oh JE, Lee KH, Park TG. Biodegradable nanoparticles containing doxorubicin-PLGA conjugate for sustained release. *Pharm Res.* 1999;16:1114-8.
15. Willis M, Forssen E. Ligand-targeted liposomes. *Adv Drug Deliv Rev.* 1998;29:249-71.
16. Ishida T, Kirchmeier MJ, Moase EH, Zalipsky S, Allen TM. Targeted delivery and triggered release of liposomal doxorubicin enhances cytotoxicity against human B lymphoma cells. *Biochim Biophys Acta.* 2001;1515:144-58.
17. BANGHAM AD, HORNE RW, GLAUERT AM, DINGLE JT, LUCY JA. Action of saponin on biological cell membranes. *Nature.* 1962;196:952-5.
18. HORNE RW, BANGHAM AD, WHITTAKER VP. NEGATIVELY STAINED LIPOPROTEIN MEMBRANES. *Nature.* 1963;200:1340.
19. BANGHAM AD, HORNE RW. NEGATIVE STAINING OF PHOSPHOLIPIDS AND THEIR STRUCTURAL MODIFICATION BY SURFACE-ACTIVE AGENTS AS OBSERVED IN THE ELECTRON MICROSCOPE. *J Mol Biol.* 1964;8:660-8.
20. Harrington KJ, Syrigos KN, Vile RG. Liposomally targeted cytotoxic drugs for the treatment of cancer. *J Pharm Pharmacol.* 2002;54:1573-600.
21. Wang CY, Huang L. pH-sensitive immunoliposomes mediate target-cell-specific delivery and controlled expression of a foreign gene in mouse. *Proc Natl Acad Sci U S A.* 1987;84:7851-5.
22. Curiel DT, Agarwal S, Wagner E, Cotten M. Adenovirus enhancement of transferrin-polylysine-mediated gene delivery. *Proc Natl Acad Sci U S A.* 1991;88:8850-4.
23. Barratt G, Tenu JP, Yapo A, Petit JF. Preparation and characterisation of liposomes containing mannosylated phospholipids capable of targeting drugs to macrophages. *Biochim Biophys Acta.* 1986;862:153-64.
24. Klibanov AL, Maruyama K, Torchilin VP, Huang L. Amphipathic polyethyleneglycols effectively prolong the circulation time of liposomes.

FEBS Lett. 1990;268:235-7.

25. Allen TM, Hansen C. Pharmacokinetics of stealth versus conventional liposomes: effect of dose. *Biochim Biophys Acta*. 1991;1068:133-41.
26. Papahadjopoulos D, Allen TM, Gabizon A, Mayhew E, Matthay K, Huang SK, et al. Sterically stabilized liposomes: improvements in pharmacokinetics and antitumor therapeutic efficacy. *Proc Natl Acad Sci U S A*. 1991;88:11460-4.
27. Gabizon A, Catane R, Uziely B, Kaufman B, Safra T, Cohen R, et al. Prolonged circulation time and enhanced accumulation in malignant exudates of doxorubicin encapsulated in polyethylene-glycol coated liposomes. *Cancer Res*. 1994;54:987-92.
28. Goren D, Horowitz AT, Tzemach D, Tarshish M, Zalipsky S, Gabizon A. Nuclear delivery of doxorubicin via folate-targeted liposomes with bypass of multidrug-resistance efflux pump. *Clin Cancer Res*. 2000;6:1949-57.
29. Versluis AJ, Rensen PC, Rump ET, Van Berkel TJ, Bijsterbosch MK. Low-density lipoprotein receptor-mediated delivery of a lipophilic daunorubicin derivative to B16 tumours in mice using apolipoprotein E-enriched liposomes. *Br J Cancer*. 1998;78:1607-14.
30. Kawakami S, Wong J, Sato A, Hattori Y, Yamashita F, Hashida M. Biodistribution characteristics of mannosylated, fucosylated, and galactosylated liposomes in mice. *Biochim Biophys Acta*. 2000;1524:258-65.
31. Chang CC, Liu DZ, Lin SY, Liang HJ, Hou WC, Huang WJ, et al. Liposome encapsulation reduces cantharidin toxicity. *Food Chem Toxicol*. 2008;46:3116-21.
32. Chen CH, Liu DZ, Fang HW, Liang HJ, Yang TS, Lin SY. Evaluation of multi-target and single-target liposomal drugs for the treatment of gastric cancer. *Biosci Biotechnol Biochem*. 2008;72:1586-94.
33. Zhang J, Jin W, Wang X, Wang J, Zhang X, Zhang Q. A novel octreotide modified lipid vesicle improved the anticancer efficacy of doxorubicin in somatostatin receptor 2 positive tumor models. *Mol Pharm*. 2010;7:1159-68.
34. Grozinsky-Glasberg S, Shimon I, Korbonits M, Grossman AB. Somatostatin analogues in the control of neuroendocrine tumours: efficacy and mechanisms. *Endocr Relat Cancer*. 2008;15:701-20.
35. Reubi JC, Kvols L, Krenning E, Lamberts SW. Distribution of

- somatostatin receptors in normal and tumor tissue. *Metabolism*. 1990;39:78-81.
36. Volante M, Rosas R, Allia E, Granata R, Baragli A, Muccioli G, et al. Somatostatin, cortistatin and their receptors in tumours. *Mol Cell Endocrinol*. 2008;286:219-29.
37. Zatelli MC, Tagliati F, Taylor JE, Rossi R, Culler MD, degli Uberti EC. Somatostatin receptor subtypes 2 and 5 differentially affect proliferation *in vitro* of the human medullary thyroid carcinoma cell line tt. *J Clin Endocrinol Metab*. 2001;86:2161-9.
38. Zatelli MC, Tagliati F, Taylor JE, Piccin D, Culler MD, degli Uberti EC. Somatostatin, but not somatostatin receptor subtypes 2 and 5 selective agonists, inhibits calcitonin secretion and gene expression in the human medullary thyroid carcinoma cell line, TT. *Horm Metab Res*. 2002;34:229-33.
39. Mato E, Matías-Guiu X, Chico A, Webb SM, Cabezas R, Berná L, et al. Somatostatin and somatostatin receptor subtype gene expression in medullary thyroid carcinoma. *J Clin Endocrinol Metab*. 1998;83:2417-20.
40. Froidevaux S, Eberle AN. Somatostatin analogs and radiopeptides in cancer therapy. *Biopolymers*. 2002;66:161-83.
41. Lemaire M, Azria M, Dannecker R, Marbach P, Schweitzer A, Maurer G. Disposition of sandostatin, a new synthetic somatostatin analogue, in rats. *Drug Metab Dispos*. 1989;17:699-703.
42. Kutz K, Nüesch E, Rosenthaler J. Pharmacokinetics of SMS 201-995 in healthy subjects. *Scand J Gastroenterol Suppl*. 1986;119:65-72.
43. Bakker WH, Krenning EP, Breeman WA, Kooij PP, Reubi JC, Koper JW, et al. *In vivo* use of a radioiodinated somatostatin analogue: dynamics, metabolism, and binding to somatostatin receptor-positive tumors in man. *J Nucl Med*. 1991;32:1184-9.
44. Froidevaux S, Heppeler A, Eberle AN, Meier AM, Häusler M, Beglinger C, et al. Preclinical comparison in AR4-2J tumor-bearing mice of four radiolabeled 1,4,7,10-tetraazacyclododecane-1,4,7,10-tetraacetic acid-somatostatin analogs for tumor diagnosis and internal radiotherapy. *Endocrinology*. 2000;141:3304-12.
45. Smith-Jones PM, Stolz B, Albert R, Ruser G, Briner U, Mäcke HR, et al. Synthesis and characterisation of [90Y]-Bz-DTPA-oct: a yttrium-90-labelled octreotide analogue for radiotherapy of somatostatin

- receptor-positive tumours. *Nucl Med Biol.* 1998;25:181-8.
46. Oberg K. Cancer: antitumor effects of octreotide LAR, a somatostatin analog. *Nat Rev Endocrinol.* 2010;6(4):188-9.
47. Chua YJ, Michael M, Zalcborg JR, Hicks RJ, Goldstein D, Liauw W, et al. Antitumor effect of somatostatin analogs in neuroendocrine tumors. *J Clin Oncol.* 2010;28(3):e41-2; author reply e3-4.
48. Weckbecker G, Raulf F, Tolcsvai L, Bruns C. Potentiation of the anti-proliferative effects of anti-cancer drugs by octreotide *in vitro* and *in vivo*. *Digestion.* 1996;57 Suppl 1:22-8.
49. Shaw RJ, Cantley LC. Ras, PI(3)K and mTOR signalling controls tumour cell growth. *Nature.* 2006;441:424-30.
50. Faggiano A, Ramundo V, Dicitore A, Castiglioni S, Borghi MO, Severino R, et al. Everolimus is an active agent in medullary thyroid cancer: a clinical and *in vitro* study. *J Cell Mol Med.* 2011.
51. Su JC, Tseng CL, Chang TG, Yu WJ, Wu SK. A synthetic method for peptide-PEG-lipid conjugates: application of octreotide-PEG-DSPE synthesis. *Bioorg Med Chem Lett.* 2008;18:4593-6.
52. Hattori Y, Shi L, Ding W, Koga K, Kawano K, Hakoshima M, et al. Novel irinotecan-loaded liposome using phytic acid with high therapeutic efficacy for colon tumors. *J Control Release.* 2009;136:30-7.
53. Yamada A, Taniguchi Y, Kawano K, Honda T, Hattori Y, Maitani Y. Design of folate-linked liposomal doxorubicin to its antitumor effect in mice. *Clin Cancer Res.* 2008;14:8161-8.
54. Arai H, Suzuki T, Kaseda C, Ohyama K, Takayama K. Bootstrap re-sampling technique to evaluate the optimal formulation of theophylline tablets predicted by non-linear response surface method incorporating multivariate spline interpolation. *Chem Pharm Bull (Tokyo).* 2007;55:586-93.
55. Ishida O, Maruyama K, Tanahashi H, Iwatsuru M, Sasaki K, Eriguchi M, et al. Liposomes bearing polyethyleneglycol-coupled transferrin with intracellular targeting property to the solid tumors *in vivo*. *Pharm Res.* 2001;18:1042-8.
56. Stroh T, Jackson AC, Dal Farra C, Schonbrunn A, Vincent JP, Beaudet A. Receptor-mediated internalization of somatostatin in rat cortical and hippocampal neurons. *Synapse.* 2000;38:177-86.
57. Huang CM, Wu YT, Chen ST. Targeting delivery of paclitaxel into

- tumor cells via somatostatin receptor endocytosis. *Chem Biol.* 2000;7:453-61.
58. Barone R, Van Der Smissen P, Devuyst O, Beaujean V, Pauwels S, Courtoy PJ, et al. Endocytosis of the somatostatin analogue, octreotide, by the proximal tubule-derived opossum kidney (OK) cell line. *Kidney Int.* 2005;67:969-76.
59. Modigliani E, Cohen R, Joannidis S, Siame-Mouro C, Guliana JM, Charpentier G, et al. Results of long-term continuous subcutaneous octreotide administration in 14 patients with medullary thyroid carcinoma. *Clin Endocrinol (Oxf).* 1992;36:183-6.
60. Lupoli G, Cascone E, Arlotta F, Vitale G, Celentano L, Salvatore M, et al. Treatment of advanced medullary thyroid carcinoma with a combination of recombinant interferon alpha-2b and octreotide. *Cancer.* 1996;78:1114-8.
61. Gabizon A, Shmeeda H, Horowitz AT, Zalipsky S. Tumor cell targeting of liposome-entrapped drugs with phospholipid-anchored folic acid-PEG conjugates. *Adv Drug Deliv Rev.* 2004;56:1177-92.
62. Koga K, Hattori Y, Komori M, Narishima R, Yamasaki M, Hakoshima M, et al. Combination of RET siRNA and irinotecan inhibited the growth of medullary thyroid carcinoma TT cells and xenografts via apoptosis. *Cancer Sci.* 2010;101:941-7.
63. Grozinsky-Glasberg S, Franchi G, Teng M, Leontiou CA, Ribeiro de Oliveira A, Dalino P, et al. Octreotide and the mTOR inhibitor RAD001 (everolimus) block proliferation and interact with the Akt-mTOR-p70S6K pathway in a neuro-endocrine tumour cell Line. *Neuroendocrinology.* 2008;87:168-81.
64. Theodoropoulou M, Zhang J, Laupheimer S, Paez-Pereda M, Erneux C, Florio T, et al. Octreotide, a somatostatin analogue, mediates its antiproliferative action in pituitary tumor cells by altering phosphatidylinositol 3-kinase signaling and inducing Zacl expression. *Cancer Res.* 2006;66:1576-82.
65. Matsumura Y, Maeda H. A new concept for macromolecular therapeutics in cancer chemotherapy: mechanism of tumor-tropic accumulation of proteins and the antitumor agent smancs. *Cancer Res.* 1986;46:6387-92.
66. Iwase Y, Maitani Y. Octreotide-targeted liposomes loaded with CPT-11 enhanced cytotoxicity for the treatment of medullary thyroid carcinoma. *Mol*

Pharm. 2011;8:330-7.

67. Guichard S, Terret C, Hennebelle I, Lochon I, Chevreau P, Frétigny E, et al. CPT-11 converting carboxylesterase and topoisomerase activities in tumour and normal colon and liver tissues. *Br J Cancer*. 1999;80:364-70.
68. Hattori Y, Yoshizawa T, Koga K, Maitani Y. NaCl induced high cationic hydroxyethylated cholesterol-based nanoparticle-mediated synthetic small interfering RNA transfer into prostate carcinoma PC-3 cells. *Biol Pharm Bull*. 2008;31:2294-301.
69. Lamberts SW, van der Lely AJ, de Herder WW, Hofland LJ. Octreotide. *N Engl J Med*. 1996;334:246-54.
70. Wu C, Huang J. Phosphatidylinositol 3-kinase-AKT-mammalian target of rapamycin pathway is essential for neuroendocrine differentiation of prostate cancer. *J Biol Chem*. 2007;282:3571-83.
71. Boulay A, Zumstein-Mecker S, Stephan C, Beuvink I, Zilbermann F, Haller R, et al. Antitumor efficacy of intermittent treatment schedules with the rapamycin derivative RAD001 correlates with prolonged inactivation of ribosomal protein S6 kinase 1 in peripheral blood mononuclear cells. *Cancer Res*. 2004;64:252-61.
72. Baker H, Sidorowicz A, Sehgal SN, Vézina C. Rapamycin (AY-22,989), a new antifungal antibiotic. III. *In vitro* and *in vivo* evaluation. *J Antibiot (Tokyo)*. 1978;31:539-45.
73. Martel RR, Klicius J, Galet S. Inhibition of the immune response by rapamycin, a new antifungal antibiotic. *Can J Physiol Pharmacol*. 1977;55:48-51.
74. Hartford CM, Ratain MJ. Rapamycin: something old, something new, sometimes borrowed and now renewed. *Clin Pharmacol Ther*. 2007;82:381-8.
75. Avellino R, Romano S, Parasole R, Bisogni R, Lamberti A, Poggi V, et al. Rapamycin stimulates apoptosis of childhood acute lymphoblastic leukemia cells. *Blood*. 2005;106:1400-6.
76. Frost P, Shi Y, Hoang B, Lichtenstein A. AKT activity regulates the ability of mTOR inhibitors to prevent angiogenesis and VEGF expression in multiple myeloma cells. *Oncogene*. 2007;26:2255-62.
77. Récher C, Beyne-Rauzy O, Demur C, Chicanne G, Dos Santos C, Mas VM, et al. Antileukemic activity of rapamycin in acute myeloid leukemia. *Blood*. 2005;105:2527-34.

78. Yatscoff RW. Pharmacokinetics of rapamycin. *Transplant Proc.* 1996;28:970-3.
79. Rouf MA, Vural I, Renoir JM, Hincal AA. Development and characterization of liposomal formulations for rapamycin delivery and investigation of their antiproliferative effect on MCF7 cells. *J Liposome Res.* 2009;19:322-31.
80. Cirstea D, Hideshima T, Rodig S, Santo L, Pozzi S, Vallet S, et al. Dual inhibition of akt/mammalian target of rapamycin pathway by nanoparticle albumin-bound-rapamycin and perifosine induces antitumor activity in multiple myeloma. *Mol Cancer Ther.* 2010;9:963-75.
81. Colby SL, Artis WM, Rietschel RL. Liposomes containing 3-n-pentadecylcatechol induce tolerance to toxicodendron. *J Invest Dermatol.* 1983;80:145-9.
82. Pencreach E, Guérin E, Nicolet C, Lelong-Rebel I, Voegeli AC, Oudet P, et al. Marked activity of irinotecan and rapamycin combination toward colon cancer cells *in vivo* and *in vitro* is mediated through cooperative modulation of the mammalian target of rapamycin/hypoxia-inducible factor-1alpha axis. *Clin Cancer Res.* 2009;15:1297-307.
83. Ghayad SE, Cohen PA. Inhibitors of the PI3K/Akt/mTOR pathway: new hope for breast cancer patients. *Recent Pat Anticancer Drug Discov.* 2010;5:29-57.
84. Niu H, Wang J, Li H, He P. Rapamycin potentiates cytotoxicity by docetaxel possibly through downregulation of Survivin in lung cancer cells. *J Exp Clin Cancer Res.* 2011;30:28.
85. Iwase Y, Maitani Y. Dual functional octreotide-modified liposomal irinotecan leads to high therapeutic efficacy for medullary thyroid carcinoma xenografts. *Cancer Sci.* 2011.
86. Harrison DE, Strong R, Sharp ZD, Nelson JF, Astle CM, Flurkey K, et al. Rapamycin fed late in life extends lifespan in genetically heterogeneous mice. *Nature.* 2009;460(7253):392-5.